FINAL REPORT

DEVELOPMENT OF AN ENGINEERING
PROTOTYPE ION MASS SPECTROMETER FOR THE
MASS ANALYSIS OF THE LUNAR ATMOSPHERE

25 September 1965

4190-6012-SU000

N 66-15618

FACILITY FORM 602

(ACCESSION NUMBER)

60

(PAGES)

CR 69480

(NASA CR OR TMX OR AD NUMBER)

(THRU)

(CODE)

4

(CATEGORY)

GPO PRICE $ _____

CFSTI PRICE(S) $ _____

Hard copy (HC) _3.00_

Microfiche (MF) __.50_

ff 653 July 65

TRW SPACE TECHNOLOGY LABORATORIES

THOMPSON RAMO WOOLDRIDGE INC.

ONE SPACE PARK • REDONDO BEACH, CALIFORNIA

FINAL REPORT

DEVELOPMENT OF AN ENGINEERING
PROTOTYPE ION MASS SPECTROMETER FOR THE
MASS ANALYSIS OF THE LUNAR ATMOSPHERE
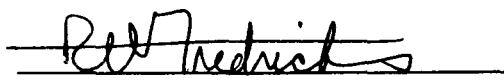

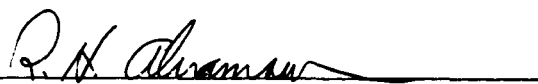25 September 1965   4190-6012-SU000
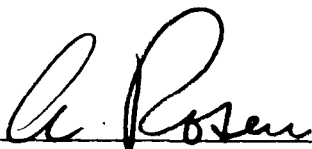

Prepared for

National Aeronautics and Space Administration
Washington, D. C.

Contract No. NASw-1022

Space Sciences Laboratory
Physical Research Division

TRW SYSTEMS
One Space Park
Redondo Beach, California

Prepared: _____

R. W. Fredricks
Project Engineer
Space Sciences Laboratory

Prepared: _____

R. H. Abramson
Member, Technical Staff
Space Sciences Laboratory

Approved: _____

A. Rosen, Director
Space Sciences Laboratory

Approved: _____

R. B. Muchmore, Director
Physical Research Division

TRW SYSTEMS

CONTENTS

ILLUSTRATIONS

1. INTRODUCTION

The purpose of the investigations summarized in this Final Report on Contract No. NASw-1022 was to study the development of an engineering prototype of a curved electrode Paul-type quadrupole electrodynamic mass filter suitable to make direct measurements on the ionized component of the lunar atmosphere. In such an experiment, the partial densities of the various ion species of scientific interest have been estimated by Bernstein, et al.(1963), Michel (1964) and Hinton and Taeusch (1964), and all model calculations yield very low ion densities. In order to measure such densities an instrument of high sensitivity is required.

The problem of far ultraviolet photoemission exists in such a device if the particle detector is to measure low count rates. In order to solve this problem we proposed to bend an electrodynamic quadrupole mass filter on a quarter-circle, thus forcing several reflections of the photons entering the entrance aperture of the mass filter before they strike the particle detector surface.

The plan of this report is as follows. In Section 2 we describe the experimental apparatus used during the program. The special oil-free vacuum system, the RF power supply, and peripheral electronics were specifically constructed under this contract. Two quadrupole mass filter structures were used in the study. One of these is an all-aluminum structure constructed by TRW Systems prior to the start date of the contract. This unit weighs approximately 3.5 pounds without electronics, and occupies a volume of some 500 cubic inches. A second quadrupole structure was constructed of magnesium alloy under this contract. This unit weighs approximately 1.5 pounds without electronics and occupies the same volume as does the TRW aluminum unit. A special power supply (breadboard) was constructed under the contract and is described in Section 2.5 and in Appendix C of this report. This laboratory unit has been designed in such a way that it provides a prototype unit from which a flight-type power supply can be evolved.

In Section 3 we discuss the physical tests to which the quadrupole mass filter (sensor) was subjected. These tests included measurement of the mass resolution, the transmission factor, and the ultraviolet

photoresponse of the curved quadrupole. It was found that the curved quadrupole structure operates in a manner consistent with both theory (Appendix A) and with the experimental results of other workers employing a straight quadrupole. The resolution and transmission were shown to satisfy the original goals of a mass resolution $20 \leq R \leq 25$ with a transmission between 20 percent $\leq T \leq 100$ percent. This means that the geometrical factor of 10^{-3} cm^2 quoted on page 2 of our original proposal No. 2730.00, dated November 1963, has been achieved, since the geometrical factor is the product of the area of the entrance aperture (5×10^{-3} cm^2) and the transmission factor ($T \geq 0.2$). It is thus a result of our study that the quadrupole structure itself has been proven to satisfactorily function as required for the lunar experiment.

The results of the ultraviolet light test in Section 3 show that if the interior of the quadrupole is blackened its photoelectric response will be negligible.

One of the major results of the physical tests outlined in Section 3 is a delineation of the problems in the path of development of a flight instrument. The major problem is that of providing a suitable, rugged and durable particle counter detector. (This is more thoroughly discussed in Section 4.) The secondary emission multiplier employed in this program as a particle detector suffers from severe contamination and handling problems. Although these problems are not insurmountable, and we feel that such a detector could be utilized, we feel our experience indicates that it is highly desirable to investigate the use of other detectors.

In Section 4 we discuss the nature of our results with respect to specific problem areas which we have isolated. Each problem area appears to be amenable to solution after further developmental work. In particular, particle detection problems are covered and our recommendations given.

Also in Section 4 we have discussed the nature of our results of physical tests of the sensor in true plasma beams. The first six months of the contract period were spent on this sort of physical testing. The reason for removing the presentation of the plasma measurements to Section 4 is that the results were ambiguous and difficult to interpret quantitatively. However, it was found that an understanding of the plasma

sheath effects is of prime importance in calibrating an ion mass spectrometer for use in an ambient plasma having a Debye length comparable to instrument dimensions. The complete investigation of plasma sheath effects would represent a program greater in magnitude than that envisaged under the present contract.

Section 5 summarizes briefly the salient results of the investigations.

Appendices A, B and C give the theory of the curved quadrupole electrodynamic mass filter, the theoretical calculations of the light intensity produced by the ultraviolet flashed light source used in the light test, and the testing and calibration procedures as well as engineering specifications of the RF power supply unit.

We have concluded that the ion mass filter of the type proposed can be engineered into a useful flight hardware item despite the developmental problems we have isolated.

2. DESCRIPTION OF EXPERIMENTAL APPARATUS

2.1 SENSOR

The sensor portion of the mass spectrometer is basically a Paul-type quadrupole electrodynamic mass filter (Paul, et al., 1958). Because of the strong focusing property of the quadrupolar electric fields, it is possible to bend the whole structure of the quadrupole about a center of curvature in the manner shown in Figure 1. It is demonstrated theoretically in Appendix A that such a curved mass filter should operate in essentially an identical fashion as does a straight Paul mass filter. The experimental evidence which verifies that the curved quadrupole sensor can be used successfully is presented in Section 3 of this report.

The design formulas for the quadrupole sensor are given in Appendix A. For any specific application of this type of sensor to planetary atmospheric/ionospheric measurements, these design formulas will yield an appropriate design in terms of dimensions, power and weight of the sensor. Since the original application of this sensor was to lunar ionospheric measurements, the design parameters were fixed by the partial densities of model lunar ionospheres and by spacecraft descent velocity. The design goals are as follows:

a) Resolution

$R = M/\Delta M = 25$ (mass line width at half peak intensity)

b) Field Radius and Radius of Curvature

In order to ensure that the device, when curved on a radius of curvature R_O, operates in the same manner as a straight device, the field radius $r_O \ll R_O$. Furthermore, because weight and RF voltage increase with increasing r_O, it is desirable to minimize r_O. As a practical (but not rigidly required) value, we have chosen $r_O = 0.4$ cm, and $R_O = 20$ cm so that $r_O/R_O = 0.02$.

c) Entrance Aperture Diameter

Since the resolution is given by $R = M/\Delta M = (r_O/d)^2$ where d is the diameter of the entrance aperture, one is forced to choose $d = r_O/\sqrt{R} = 0.4/5 = 0.08$ cm.

d) Oscillator Frequency

The voltage and power of the RF power supply increase with increasing frequency, while the minimum length of the quadrupole structure is inversely proportional to the frequency. As a suitable compromise, the RF supply frequency was chosen to be $f = 1.0$ megacycles.

e) Voltage Requirements

In order to cover the mass range from 14 amu to 83 amu, the peak RF voltage must be variable from at least 16 to at most 100 volts peak. The power supply is described in Section 2.5.

f) Spectrometer Length

The path length was fixed by the choice of a curved geometry of a 90 degree circular sector; $L = R_o \theta_o = 20 \times \pi/2 \simeq 31.4$ cm.

g) Pre-Acceleration

No pre-acceleration was provided, and the sensor was operated in ion beams up to ~ 100eV kinetic energy without apparent difficulty.

2.2 DETECTORS

The sensor, or quadrupole structure, was operated with a wide-open exit aperture. Hence the exit aperture was effectively the field diameter $2r_o = 0.8$ cm. Two detectors were used to collect the mass-analyzed ions emerging from the sensor. These were:

a) Faraday Cup

A Faraday cup collector was used at high ion beam intensities. This consisted simply of a copper cup collector of sufficient diameter (7/8 inch) to intercept all emerging ions. This cup could be moved back and forth in the axial direction.

b) Secondary Emission Multiplier

For detection of mass analyzed currents less than a few times 10^{-12} ampere, a secondary electron multiplier was employed. This SEM device was the dynode chain structure of the RCA 7746 photomultiplier tube. The input to the dynode structure had been altered such that it consisted of a flat metal plate with a 3/8 inch by 5/8 inch rectangular aperture. This plate was tied electrically to the first dynode. The dynodes in this structure are Cu-Be alloy, and therefore highly sensitive to hydrocarbon and other gaseous contamination. This structure under ideal conditions is capable of producing gains of up to 10^6.

2.3 VACUUM SYSTEM

The high vacuum system used throughout the testing is a Consolidated Vacuum Corporation 2 inch mercury system. This included type MHG40 mercury diffusion pump, BCRU-20 water cooled chevron baffle, and BC-20 liquid nitrogen chevron baffle. The pumping system is coupled to the vacuum chamber through a type VCS-21 2-inch gate valve. The liquid nitrogen baffle is continuously filled by a CVC type BC 013 automatic liquid nitrogen filling system. The high vacuum pump is backed by a standard fore pump with a liquid nitrogen trap in the foreline to prevent fore pump oil vapor from getting into the diffusion pump. The base pressure achieved with this system was 5×10^{-6} torr. To prevent oil contamination during rough down, a Varian Associates model 941-5610 Vac-Sorb cryogenic pump is used to rough the system to around 50 microns at which time the diffusion pump takes over.

2.4 ION SOURCE

The ion source consisted of a CHA Industries (Carl Hermann Associates) Type IG100K ionization gauge with the grid and collector electrically tied together. The filament is run at approximately 6 amperes using a battery voltage source and one side of the filaments tied to the system ground. The grid and collector are run at +65 volts. Gas is leaked into the tube by a Granville Phillips model 9101-M-L variable leak diaphragm valve and a glow discharge is set up in the ion tube. Ions from this glow discharge leak out through a 20 mil aperture into the vacuum chamber. The ion source is capable of producing an average beam current of around 3×10^{-8} ampere/cm^2. Associated with the ion source is a beam analyzing magnet and slit system. The analyzing magnet was used in all of the transmission measurements to reject any contaminant masses that could be present in the ion source. The magneti-slit system has a resolution of one mass unit. The ion source and analyzing magnet were arranged so that the magnet could be removed and ions injected directly into the vacuum chamber.

2.5 ELECTRONICS

Appendix C contains a circuit diagram of the RF-DC power supply. The main features of the unit are a crystal controlled 1 Mc/sec oscillator, a buffer amplifier, a push-pull transformer coupled output stage and a

6

feedback network for a high degree of stability. The DC voltage is obtained by rectifying the output tank circuit RF voltage and picking off the desired amount by the slope control pot in the rectifier load circuit. Two such rectifier circuits are used, one for each set of quadrupole rails. As shown on the circuit diagram the RF amplitude is monitored by measuring the total DC voltage developed across the resistive load of the rectifier. A 1K decoupling resistor is placed between this monitor point and the rectifying diode. The RF amplitude was calibrated by the use of Fluke thermal transfer converters. The following summarizes the specifications of the unit under normal room ambient temperature conditions and laboratory line variations:

a) Output Frequency

1 Mc/sec crystal controlled, drift less than 2 cps in 8 hours

b) Output Amplitude

Continuously variable from 2 to 100 volts peak for RF

DC continuously variable from 0 to 0.20 times the peak AC voltage

c) Output Amplitude Stability - RF and DC

Better than 0.01 percent/hour at 100 volts peak and 0.05 percent/hour at 10 volts peak

d) Output Amplitude AC Accuracy

Calibrated against Fluke thermal transfer converters to better than 0.05 percent at 55 volts peak

e) Tracking Linearity (Rectified DC Voltage)

Better than 0.05 percent from 20 to 55 volts peak RF.

Details of calibration of this unit are given in Appendix C.

3. PHYSICAL TESTS

The physical tests of the sensor consisted of resolution and transmission measurements under a wide variety of conditions, and a test of response to ultraviolet light. A wealth of data has been acquired, and the portions selected for presentation in this report are felt to demonstrate the operation of the curved quadrupole mass filter most typically, as well as to point out which areas present unresolved problems in the development of a useful flight-qualified instrument.

3.1 RESOLUTION MEASUREMENTS

The theoretical resolution $R = M/\Delta M$ of the sensor as given in Appendix A is fixed by the geometrical factor r_o/d, i.e., the ratio of the exit aperture radius to entrance aperture diameter. Thus, for the dimensions selected the quadrupole sensor under study has a theoretical resolution of 25. The design formula $R = (r_o/d)^2$ in reality gives the theoretical upper limit of achievable resolution of an ideal sensor when the ratio of d-c to RF peak electrode voltage is optimum, that is $U/V = 0.16784$.

In practice, the resolution can be altered by reducing the "slope" $U/V < 0.16784$. In Figure 2 we show the so-called "neck-tie" stability diagrams for the two masses, argon (40 amu) and CO_2 (44 amu). The ordinate is the DC electrode voltage U and the abscissa is the peak RF voltage V. The regions bounded by the curves and the abscissa represent the sets of values (U, V) for which any ion of the mass in question is guided through the quadrupole field on a trajectory which is sufficiently stable to not intersect the electrode surface. The value $U/V = 0.16784$ represents the unique point of apex of the neck-tie region.

It is obvious from a study of Figure 2 that operation of the voltages in a fixed ratio $U/V < 0.16784$ will yield lower resolutions with decreasing ratio. Clearly, the transmission factor (ratio of incident to emerging ion flux) of the sensor will be a function of the ratio U/V. In Figure 3 we show the behavior of relative transmission versus slope (U/V) for the mass filter used in these studies. The transmission can be seen to drop sharply as $U/V \longrightarrow 0.16784$. It follows that slope settings must be accurately regulated in the operation of such a device for resolutions near the maximum,

8

because of the steep slope of the transmission curve in this region. Small errors in the actual slope setting in this region can lead to large errors in absolute mass peak intensity measurements without leading to any appreciable difference in resolution.

The resolution measurements were made using both the Faraday cup and the electron multiplier detectors. Measurements were made using argon (40 amu) and N_2 (28 amu) ion beams. Typical resolution curves taken using a Faraday cup detector are shown in Figures 4, 5 and 6. Figure 4 shows the resolution of an ion beam containing both argon and CO_2. The mass separation is 4 amu for these two ions, and one can see that the mass filter was quite capable of resolving them with R = 20. Figures 5 and 6 show two resolved mass peaks, both argon. Figure 5 shows the result of a slope setting U/V = 0.153 while Figure 6 is the result of a slope setting 0.11. One can see that the slope 0.153 produces a resolution close to the design value of 25, while the lower slope 0.11 produces a poor resolution of 11 .

In Figure 7 we show a similarly resolved mass peak using an electron multiplier detector. The slope setting was again U/V = 0.153. Here, the apparent resolution is R = 32, which is greater than the maximum theoretical design limit of 25. Since the front end of the electron multiplier is tied to -4 kV, it is apparent that the presence of the multiplier can influence conditions at the exit aperture. Since the resolution $R = (r_o/d)^2$, where r_o is the exit aperture radius, the ion focusing effects of the -4 kV potential may well make an effective exit aperture radius $r_{eff} > r_o$ and thus explain the increased resolution. However, the fringe and terminal field effects at the exit aperture defy calculation, and the experimental result must stand by its own strength. This effect on resolution appears as an area for future, more thorough study.

3.2 TRANSMISSION MEASUREMENTS

The absolute transmission factor of the quadrupole mass filter is defined as the ratio of the current collected by a detector located behind the exit aperture of the device to the current passing through the entrance aperture. In the case where a simple Faraday cup collector is used as a detector, collector currents greater than 10^{-12} ampere can be detected

conveniently by a standard laboratory micromicroammeter. When a secondary electron multiplier detection system is used (for exit currents less than 10^{-12} ampere), the gain of the dynode structure must be known in order to relate the measured current to the transmission. In Figure 8 we show the experimental configurations; the results of transmission measurements are discussed below.

3.2.1 Transmission Measurements Using the Faraday Cup

The collector is a copper Faraday cup of diameter 7/8 inch placed typically a few thousandths of an inch behind the exit plane of the quadrupole structure. The measurements were made using back-biasing voltages between zero and -10 volts on the cup. It was determined that secondary electron emission was unimportant since there was no observed effect on the collection efficiency of the cup as a function of back-biasing voltage. For this reason, the measurements presented in this report were made with no back-bias on the cup. The current collected by the cup was measured by a Millivac MV07C micromicroammeter which has a lower sensitivity limit of 10^{-12} ampere.

The current through the entrance aperture of the quadrupole mass filter was measured by placing the probe shown in Figure 8 in front of the aperture. To eliminate uncertainties in the incident ion beam density profile (radially), the centers of the probe aperture and quadrupole entrance aperture were carefully aligned. The transmission of the quadrupole was then simply computed as the ratio of the Faraday cup collector current to the front-end probe current, the latter corrected for slight mismatch in probe and quadrupole aperture areas.

During transmission measurements, the RF electrode voltage was preselected to correspond to the peak of the mass line, while the slope U/V was adjusted to give a variable resolution. To ensure a monospecific ion beam at the entrance aperture, an analyzing magnet was used in front of the ion source so as to reject any contaminant masses.

The transmission results presented in the table on the next page are for an argon (40 amu) ion beam at 65 eV. These results are typical of the Faraday cup transmission measurements made using ion beams up to ~80 eV.

10

Transmission (percent)	Slope U/V	Resolution
77	0.151	20
63	0.153	25
56	0.155	>25

3.2.2 Transmission Measurements Using an Electron Multiplier

The secondary electron multiplier detector (SEM) has been discussed in Section 2.2b. The technique used to measure the spectrometer aperture current was the same as the probe method described in Section 3.2.1 above for the Faraday cup detector. Thus, the electron multiplier was used as a current amplifier for the transmission measurements.

In order to compute the transmission using the entrance aperture current and the electron multiplier output current, it is necessary to know the overall gain of the dynode chain of the electron multiplier. The transmission is given by

$$T = I_m / \overline{G} I_p$$

where I_m is the output current of the final dynode (anode) of the SEM, I_p is the probe current (equal to the current through the entrance aperture of the quadrupole) and $\overline{G}$ is the average gain of the SEM. This gain is

$$\overline{G} = (6.25 \times 10^3) C \overline{V}$$

where C is the combined SEM anode and preamplifier input capacitances in $\mu\mu$f, while $\overline{V}$ is the average pulse amplitude in millivolts as measured on a TMC 400-channel pulse height analyzer. Figure 9 shows a pulse height (differential) distribution taken using a low intensity beam of molecular nitrogen ions. One can see from the amplitude spectrum that the distribution is sufficiently broad to necessitate a numerical integration to obtain the value of $\overline{V}$ used in the gain equation. (This is a consistent procedure since the metering circuit measures the average current from the SEM.) The average value $\overline{V}$ is calculated from

$$\overline{V} = \left[\int_{V_{min}}^{V_{max}} n(V) V \, dV \right] \bigg/ \left[\int_{V_{min}}^{V_{max}} n(V) \, dV \right]$$

11

where $n(V)$ is the number of pulse heights between V and $V + dV$ (the ordinate in Figure 9), and V_{max}, V_{min} are defined in Figure 9.

For the ratio $U/V = 0.153$, the transmission for an N_2 ion beam using the SEM detector was calculated to be 27 percent. For the same beam, using a Faraday cup collector, this transmission was 26 percent. Also, the transmission versus slope (U/V) for both detectors have the same shape (see Figure 3). This shows that the -4 kV potential applied to the SEM front plate did not significantly influence the transmission of the quadrupole mass filter since the Faraday cup was not biased to such a potential.

3.2.3 Problem Areas in Transmission Measurement

During the course of our investigations it was found that very significant problems are encountered when one desires to perform absolute transmission measurements on the quadrupole mass filter. The major problem arises in maintaining mechanical tolerance in the alignment of the mass filter axis-of-symmetry and the center of the entrance aperture. This alignment is accomplished by a careful machining of the bearing surfaces between the case of the quadrupole structure and the end plate containing the entrance aperture. Since this technique of alignment requires a very tight fit of the bearing surfaces, the manifold disassembly of the front end plate and case during the course of experimental modifications undoubtedly destroys the close tolerance required for proper alignment. When this tolerance is degraded, the entrance aperture is no longer centered on the axis of the quadrupole field. The off-axis injection of ions leads to a degradation of the transmission factor since many of the ions which would have traversed the device on trajectories not intercepting the electrode surfaces, were they injected symmetrically about the quadrupole axis, are forced to execute trajectories which do intercept the electrodes.

However, the problem of alignment only affects the absolute transmission, which in turn determines the sensitivity threshold of the mass filter (the minimum detectable flux). An absolute calibration of the mass filter and detector system is possible even for a misaligned instrument. This problem has been isolated, is understood, and can be easily resolved by a rigid design to maintain the alignment tolerances, thus optimizing the

absolute transmission at a given resolution. Therefore no expensive and time-consuming effort was made to remachine the bearing surfaces during this program.

3.3 ULTRAVIOLET LIGHT TEST

Because of the desired high sensitivity of the mass filter, the photo-electric response of the curved electrode quadrupole structure and detector must be known. The electron multiplier dynodes are of Cu-Be, a surface known to be a good photoelectron emitter with a work function perhaps as low as 4 eV. Hence, ultraviolet wavelengths below about $\lambda = 3000 \overset{o}{A}$ can produce photoelectric emission from the first dynode, with subsequent multiplication in the dynode chain. Such photocurrents could overwhelm the desired ion count rates.

The experimental arrangement shown in Figure 10 was used to study the ultraviolet light response of the mass filter. A TRW Model 27A Continuum Radiation Source was used. This source approximates a blackbody radiator at an equivalent temperature of $4.8 \times 10^4 \, ^oK$. A spherical mirror reflects and images this source at a distance D = 17 inches from the quadrupole entrance aperture. The spectrum of the source is cut off below $1200 \overset{o}{A}$ by the LiF window. The source is basically a vacuum spark discharge producing pulses of the type $I_o \exp(-t/t_o)$ where $t_o \simeq 2 \, \mu sec$ (rising to I_o in $0.4 \, \mu sec$). Debris is ejected by this source which builds a coating on the spherical mirror so that the reflectance is degraded from near unity to about 0.1 in 20 pulses and must be cleaned. Because of this feature the photoelectric response of the electron multiplier was displayed on an oscilloscope and photographed rather than pulse height analyzing the signal.

The actual test consisted of first placing the electron multiplier in the position shown in Figure 10. A mask containing an aperture of 0.031 inch diameter (equal to that of the entrance aperture of the mass filter) was placed in front of the first dynode. The light pulse from the source was then triggered, producing a voltage pulse at the output of the electron multiplier (corrected for a 14.4-to-1 attenuator) of 403 volts. The multiplier was then mounted behind the quadrupole mass filter, whose aperture was positioned in the same location as the aperture in the multiplier mask in the previous test. The light source was again triggered, but no visible

13

pulse at the output of the electron multiplier was observed above the noise level. This noise level was 2 millivolts. We thus conclude that the light transmission of the curved quadrupole structure has an upper limit $\bar{\tau} \simeq 2 \times 10^{-3}/4 \times 10^2 = 5 \times 10^{-6}$, or a lower limit of about 2×10^5.

In order to relate the measurement described above to the photo-electric response of the instrument, we use the estimate of quantum yield factor of the Cu-Be dynode surface derived from the photoresponse of the electron multiplier in the first light test. The voltage pulse was developed across a capacitor of 10 $\mu\mu$f. Thus, the total charge at the multiplier output due to photoelectrons is $Q = C\bar{V} = 10^{-11} \times 4 \times 10^2 = 4 \times 10^{-9}$ coulombs. This implies that the number of photoelectrons emitted at the first dynode was

$$n_e \simeq \frac{C\bar{V}}{e\bar{G}} = \frac{4 \times 10^{-9}}{1.6 \times 10^{-19} \times 10^3} = 2.5 \times 10^7 \text{ electrons}$$

where we have used a multiplier gain $\bar{G} = 10^3$. The number of photons incident at the first dynode is shown in Appendix B to be $n_{ph} \leq 4 \times 10^{10}$ photons for a 2 μsec light pulse. The quantum yield is then

$$\bar{\gamma} = \frac{n_e}{n_{ph}} \geq \frac{2.5 \times 10^7}{4 \times 10^{10}} = 6 \times 10^{-4} \text{ electron/photon}$$

It is possible now to compute the background count rate, in the presence of the solar ultraviolet spectrum, to be expected as an upper limit in the instrument tested. According to Hinteregger's (1961) the total number of ultraviolet photons in the solar spectrum below 3000 $\overset{o}{A}$ is $\Phi_o \simeq 2.6 \times 10^{15}$. The maximum photoelectric count rate looking directly at the sun would be

$$CR \gtrsim \Phi_o (\pi d^2/4) \bar{\gamma} \bar{\tau} \text{ (counts-sec}^{-1})$$

$$\gtrsim 3.9 \times 10^4 \text{ counts-sec}^{-1}$$

This count rate due to photoelectrons is intolerably high. However, one must realize that: (1) the flux Φ_o will be reduced at least an order of magnitude by reflection from a lunar surface; (2) the value $\bar{\tau} \lesssim 5 \times 10^{-6}$ is first of all an upper limit, and second, was established for a quadrupole structure consisting of bare, unblackened metal. By blackening the interior of the mass filter one can expect a further reduction of the diffuse

14

reflection coefficient of from 10^{-2} to 10^{-3} per reflection. Since at least two reflections are required for any photon to reach the first dynode of the multiplier, we can safely assume that the upper limit of 5×10^{-6} transmission will be reduced by 10^{-4} to 10^{-6} by appropriate blackening of the reflecting surfaces alone. Hence, it appears on the basis of the light test that photoelectric problems will be easily resolved for this instrument, and count rates due to the photoelectric effect can be reduced at least to the cosmic ray background by standard, known blackening techniques.

4. DISCUSSION OF RESULTS

4.1 RESOLUTION VERSUS TRANSMISSION

The investigations of resolution and transmission made in the course of this program show that the curved electrode spectrometer can be successfully used, and that its resolution and transmission are in general experimental agreement with the theory. However, if one operates such a mass filter near the theoretical upper limit of mass resolution, it is apparent from curves such as Figure 3 that the ratio of DC to RF electrode voltage, U/V, must be very accurately known and maintained in order to ensure a good absolute measurement of the mass peak intensity.

As an example, consider the table of transmission versus ratio U/V in Section 2.2a. A change in ratio $\Delta(U/V) = 0.155 - 0.151 = 0.004$ is equivalent to a ± 0.5 percent regulation in U and V. However, the transmission varies from 77 percent to 56 percent, or nearly a 32 percent change in transmission. Thus, a ± 2 percent regulation of voltages, while sufficient to maintain adequate resolution, is totally inadequate to maintain acceptable accuracy in absolute mass peak intensity.

With the foregoing in mind, we feel it is necessary to thoroughly study the whole question of transmission, resolution and entrance aperture size in order to properly design a quadrupole mass filter for a specific flight environment. It is possible to trade off the three parameters, resolution, transmission and output ion current in many ways, and thus avoid the absolute peak intensity problem. This represents a defined area for much future developmental work.

4.2 RESOLUTION DEFINITIONS

The theoretical and experimental resolutions quoted in the present report are defined as the full width of a mass peak at one-half maximum intensity (FWHM). When one is confronted with the task of experimentally measuring the peaks of, say, the isotopes Ne^{20}, Ne^{21}, and Ne^{22} which occur in the abundance ratio 1.15:0.0038:0.12, a mass filter of resolution 20 FWHM is adequate to resolve Ne^{22} from Ne^{20} (see Figure 4 for the A^{40}-CO_2 mixture). However, the Ne^{21} peak intensity is only 3.3×10^{-3} times the Ne^{20} peak and is 1 amu away. It is clear that the resolution

of 20 FWHM is inadequate to resolve this peak, since the wing of the Ne^{20} line has an intensity vastly greater than this at an equivalent mass of 21 amu.

In order to specify the FWHM value of resolution required for determining a specific pair of mass peaks of known and disparate intensities, a study of the shape of a mass peak far out in the wings of the line must be performed. We recommend this as a very important area of future research and development of the quadrupole mass filter, requiring a parallel development of very sensitive detectors capable of very low count rates, with low background noise.

4.3 DETECTOR PROBLEMS

As a result of the present development program, we have found that the use of standard copper-beryllium secondary emission multipliers as particle detectors is unsatisfactory from a utilitarian standpoint. While there is no doubt that this SEM can be successfully employed in the fashion envisaged at the initiation of the present program, it represents the least trustworthy and most difficult-to-handle portion of the instrument.

The most formidable problem we have encountered with the SEM detector is its extreme susceptibility to gain degradation. The copper-beryllium dynode surfaces are quite unstable, being easily contaminated when exposed to any environment other than a hard vacuum (or perhaps an inert gas). The experimental program carried out under the present contract required frequent cycling of the vacuum system between vacuum and room air conditions. This was required any time a modification of the mass filter or electronics located within the vacuum system was effected. Such cycling and subsequent exposure of the SEM to room air caused gradual degradation of the gain until the SEM became useless. Although we provided a relatively oil-free vacuum system, it is apparent that the SEM is so subject to contamination and unexplainable gain decrease to warrant considering other detector systems to replace it. The complicated handling procedures to which we resorted, such as immediately placing the SEM in a plastic bag containing helium upon dismounting it in air, were partially successful, but at best we feel the Cu-Be SEM to be much less reliable as a particle counter than one really desires in flight hardware.

17

As a replacement for the Cu-Be SEM as a particle counting detector, we feel that the Channeltron Electron Multiplier presents the best alternative. The use of a channeltron detector is a most appealing area of future development. Although these devices are limited to count rates not exceeding 5×10^5 sec^{-1}, they are apparently stable against contamination from most sources other than water vapor, an easily controlled impurity. They can be used conveniently at gains of more than 10^6. The greatest drawback of the channeltron is its inability to function as a current detector (current amplifier). However, this limitation can very likely be minimized by a clever experimental design. For the very low ion densities expected in a lunar atmosphere, the limitation to counting does not appear to present serious objections to the use of a channeltron detector.

Another alternative to the use of the SEM detector is a crystal scintillator-photomultiplier detector. Here, however, there are high voltage problems since the ions emerging from the spectrometer must be post-accelerated by some 10 to 40 kV to produce sufficient secondary electrons to stimulate the crystal. Such high voltages always present breakdown and consequent reliability problems in a flight instrument. However, such crystal scintillator-photomultiplier systems have been developed and flown successfully (ogilvie, et al., 1963; Bame, et al., 1964). The possibility of using such a detector system presents an area of future developmental study.

A problem common to all of these detector systems is the pulse height distribution due to internal detector noise. The lowest noise-producing configuration is the most desirable, all other problems being assumed equal. The noise properties of these various detector systems require thorough study in any future development program. Because of the severe gain degradations and instabilities of the SEM detector, it was not possible to do a meaningful study of the internal noise problems in this detector system under the present contract. However, with the careful handling techniques developed at the end of the study period, it should be possible to study the noise distribution in a high-quality SEM operated at high gains ($\overline{G} \sim 10^6$) and thus select an appropriate pulse-height bias level.

4.4 PLASMA SHEATH EFFECTS

In the initial six months of the contract period, we studied the performance of the quadrupole mass filter in the presence of a streaming plasma containing both positive ions and electrons. The plasma beams were produced by bombardment ionization, extracted at low voltages (25 ev to 100 ev), and neutralized by electrons emitted by a hot wire filament. These beams had the charge-neutral properties of a plasma. The ion and electron temperatures are typically $T_i \sim 100 - 300\ ^{\circ}K$, $T_e \sim 2 - 5 \times 10^3\ ^{\circ}K$. Ion currents up to a $\mu amp/cm^2$ at 20 to 100 ev streaming energy were available. Ion densities of 10^6 to $10^8\ cm^{-3}$ were produced.

It was found that the resolution properties of the quadrupole mass filter were the same as those subsequently measured using ion beams and reported in Section 3.1. However, the transmission factor measurements using a plasma beam were found to be ambiguous and in many cases appeared inconsistent. The transmission factor was found to depend on the beam conditions, namely beam current density and electron temperature. This qualitative dependence was analyzed, and it is our conclusion that plasma sheath effects were responsible for the ambiguities and otherwise inconsistent transmission measurements.

We base this conclusion on a consideration that in the plasmas used, the densities and electron temperatures were such that the Debye length $\lambda_D = (kT_e/4\pi n e^2)^{1/2}$ was in the range $0.01 < \lambda_D < 0.40$ centimeter. Thus, the Debye length was always on the order of or smaller than the dimension of the quadrupole and even smaller than the diameter of the entrance aperture (0.08 cm). Since plasma sheaths develop over dimensions on the order of a few Debye lengths, the actual ion currents to the aperture of the mass filter were subject to strong and variable sheath electric fields. Measurement of the ion current by means of a standard Faraday cup of cross section 4 inches square cannot under these sheath conditions be accurately related to the collector current measured by the mass filter.

We felt that the plasma sheath effects represented, by themselves, a research problem of magnitude greater than the scope of the original development program under the present contract. For this reason, among

others, it was decided to construct a new, oil-free vacuum system and a pure ion beam source for use in our contractual program. Since the Debye length expected in any model lunar atmosphere presently acceptable is greater than 10 meters, plasma sheath effects should be negligible. Therefore, it is appropriate to use pure ion beams for the purpose of testing and calibration of a lunar mass spectrometer.

However, we consider the studies carried out in the short Debye length plasmas of great qualitative value. The results of these experiments show very conclusively that an ion mass spectrometer performs significantly differently in plasmas of Debye length short compared to apparatus dimensions. It is manifestly clear that calibrations made of such an ion mass spectrometer by means of pure ion beams are false and misleading if one envisages the use of such a mass spectrometer in a plasma sufficiently dense and cool to have Debye lengths on the order of instrument dimensions. As a result of our studies, we recommend that mass spectrometers be calibrated under conditions consistent with the plasma environment to be anticipated in the actual flight (or laboratory) experiment.

5. SUMMARY

An ion mass spectrometer of the Paul type, and having a one-quarter circular geometry has been shown to have the mass resolution and transmission factor properties expected from both theoretical considerations and from results of laboratory experiments using linear quadrupole structures (Brubaker and Tuul, 1964).

The spectrometer has been found to operate satisfactorily at high incident ion currents where a simple Faraday cup current detector and standard laboratory micro-microammeter provide adequate measurements.

At lower current densities, where either current amplification or pulse counting modes of detection are necessary, the use of a secondary electron multiplier (SEM) has been studied. As a result of this study, it is recommended that another detector system be considered because of gain degradations and handling difficulties of the type of SEM structure used in the present program, which is sensitive to a multitude of surface contaminants.

The spectrometer has been subjected to an ultraviolet light test which yielded an upper limit to the light transmission of the unblacked, curved structure. A much lower upper limit for a blackened structure is expected, and it appears on the basis of this light test that no photoelectric count rate above cosmic ray background is reasonably expected for such a suitably blackened quadrupole.

The operation of the ion mass filter in an ambient plasma having Debye lengths comparable to instrument dimensions has been studied. It has been found that in this type of plasma, the sheath effects present serious calibration problems. However, for reasonable model lunar atmospheres, sheath effects will be unimportant because of the very large Debye length.

Recommendations for areas of future concentrated research and development have been outlined. The area which presents the greatest developmental problem is that of high sensitivity particle detection systems for use at low ambient ion flux densities.

It is our conclusion that the principle of the curved rail ion mass filter has been demonstrated; that an instrument of moderate resolution and useable transmission factor can be successfully constructed; that the sensitivity of such an instrument will depend upon the development of a low noise, low count rate particle detector, which represents the major obstacle to the successful development of an adequate flight instrument; that the electronics, such as power supplies, amplifiers and logical circuitry represent only routine, state-of-the-art engineering developments; that our present information is sufficient to conclude that an instrument of total weight of 5 to 6 pounds, with a volume requirement of perhaps 600 cu in (10 x 10 x 6 inches), and consuming a power of less than 5 watts is feasible.

REFERENCES

Bernstein, W., R. W. Fredricks, J. L. Vogl and W. A. Fowler, "The lunar atmosphere and the solar wind," Icarus 2, 233-248 (1963).

Brubaker, W. M. and J. Tuul, "Performance studies of a quadrupole mass filter," Rev. Sci. Instr. 35, 1007-1010 (1964).

Hinton, F. L. and D. R. Taeusch, "Variation of the lunar atmosphere with the strength of the solar wind," J. Geophys. Res. 69, 1341-1348 (1964).

Michel, F. C., "Interaction between the solar wind and the lunar atmosphere," Plan. and Space Sci. 12, 1075-1091 (1964).
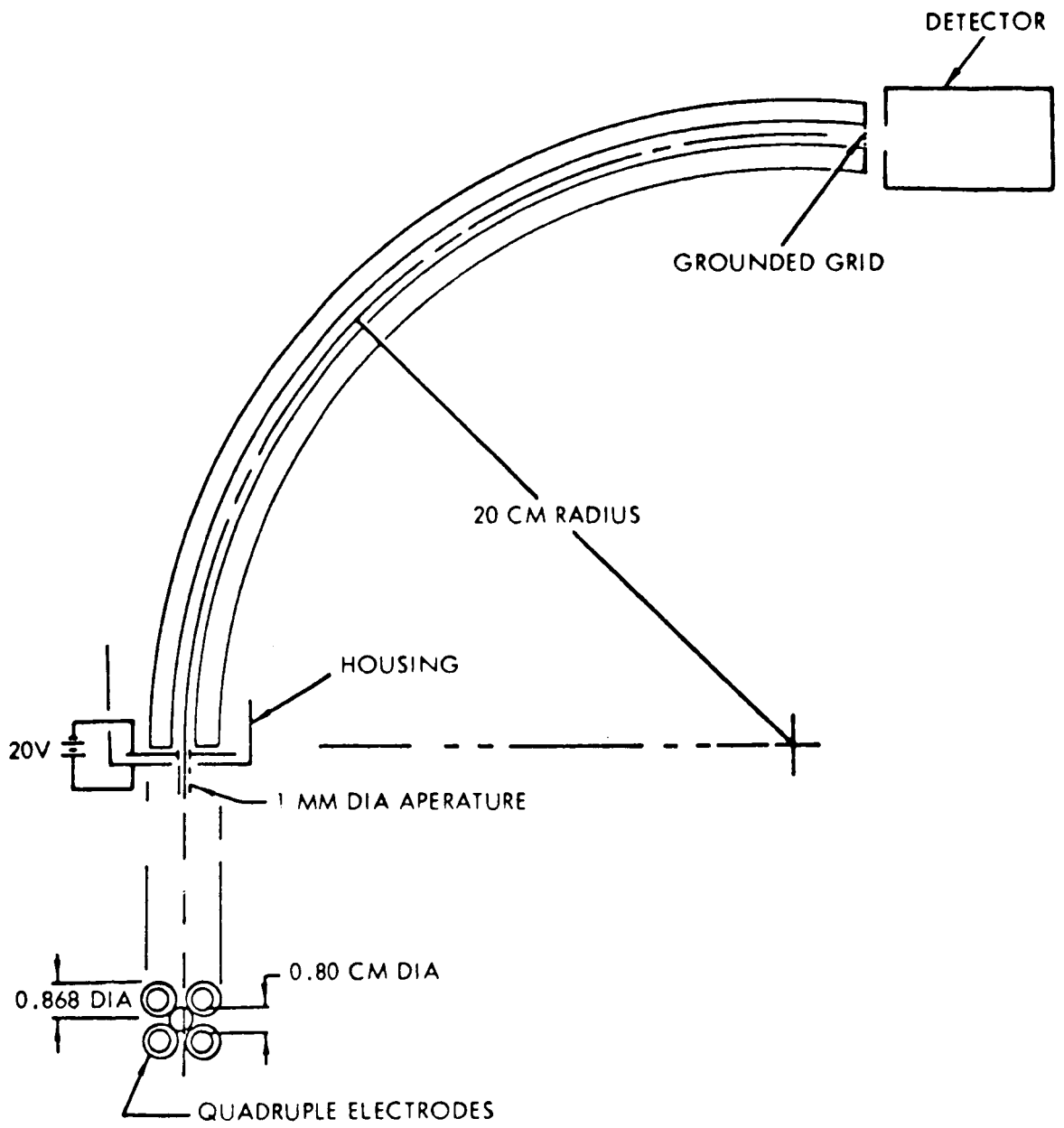
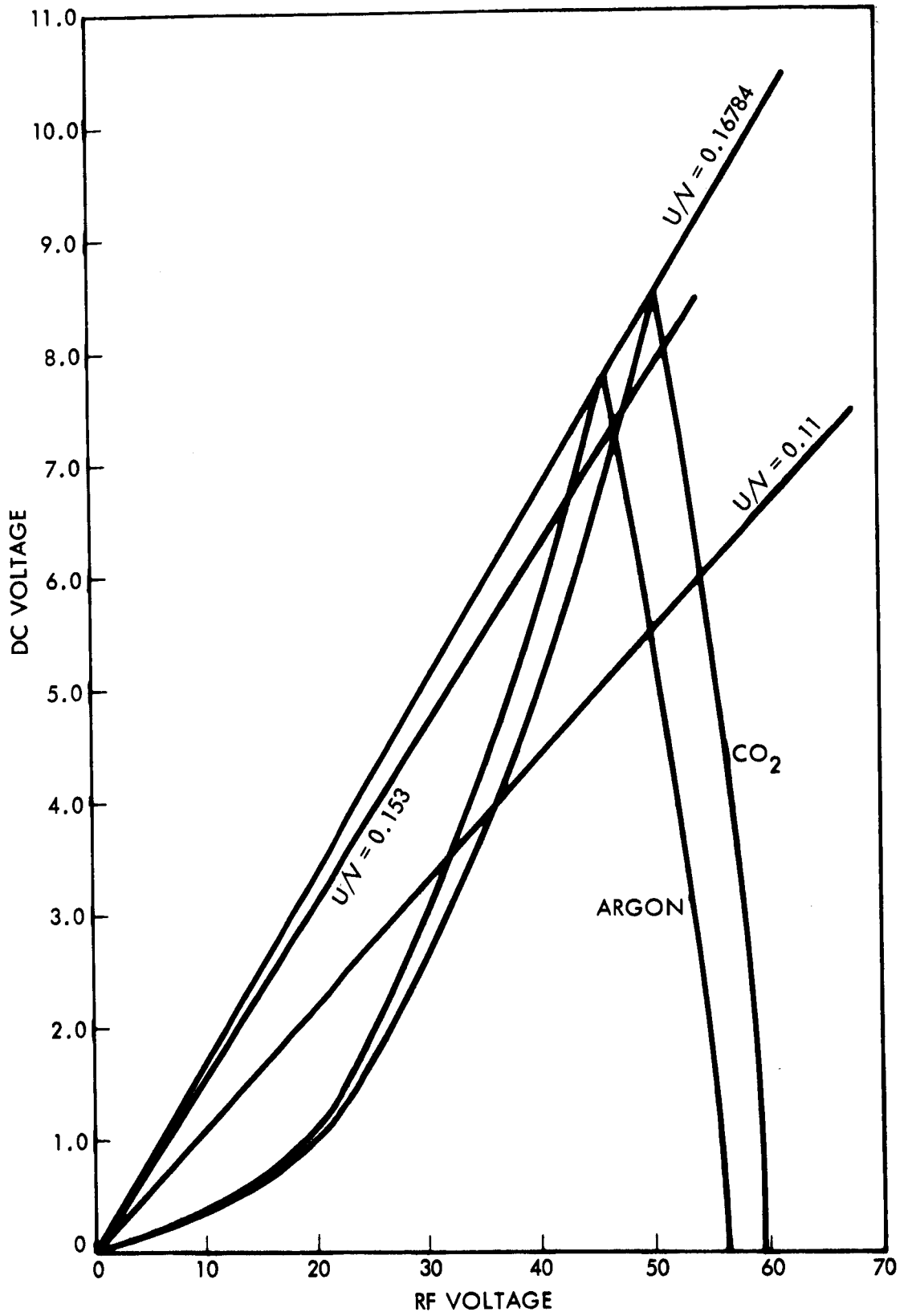Figure 1. Curved Electrode Geometry for Quadrupole Spectrometer

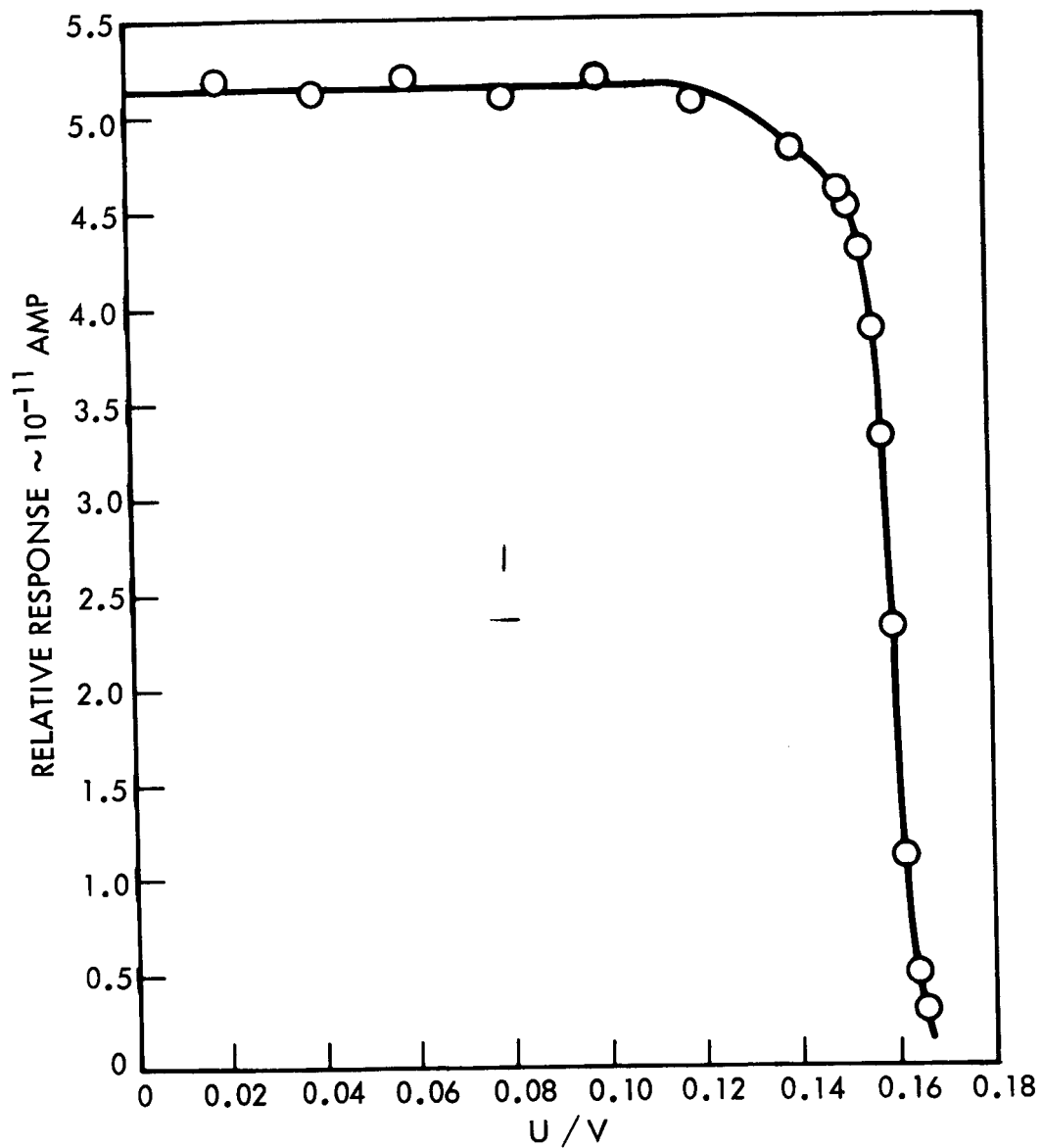Figure 2.   Stability diagram for Argon and
Carbon Dioxide

Figure 3. Relative Response of Quadrupole Spectrometer as a
Function of U/V Ratio for Argon Ions
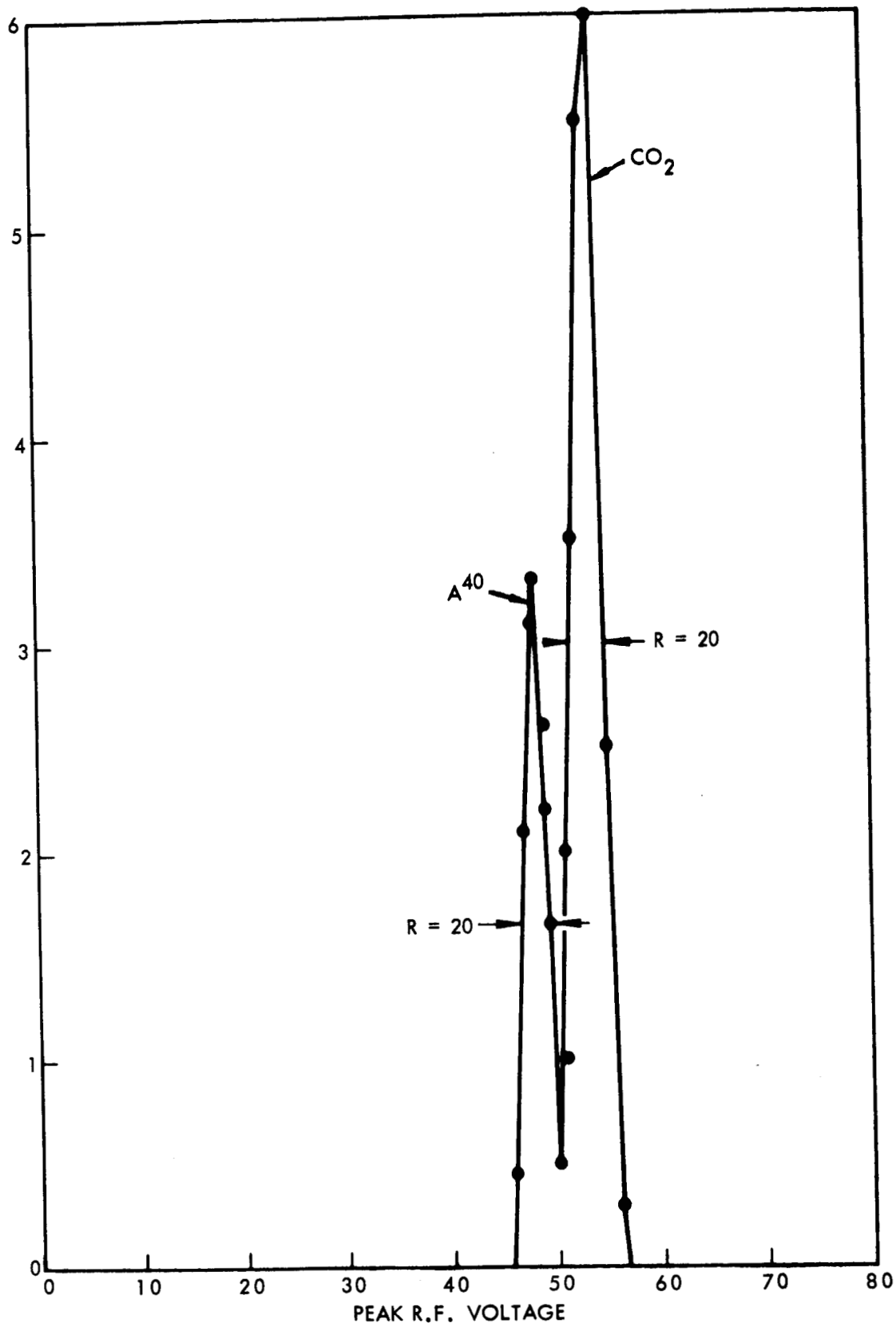
Figure 4.   Argon-CO_2 Resolutions Curve
(Faraday cup detector)
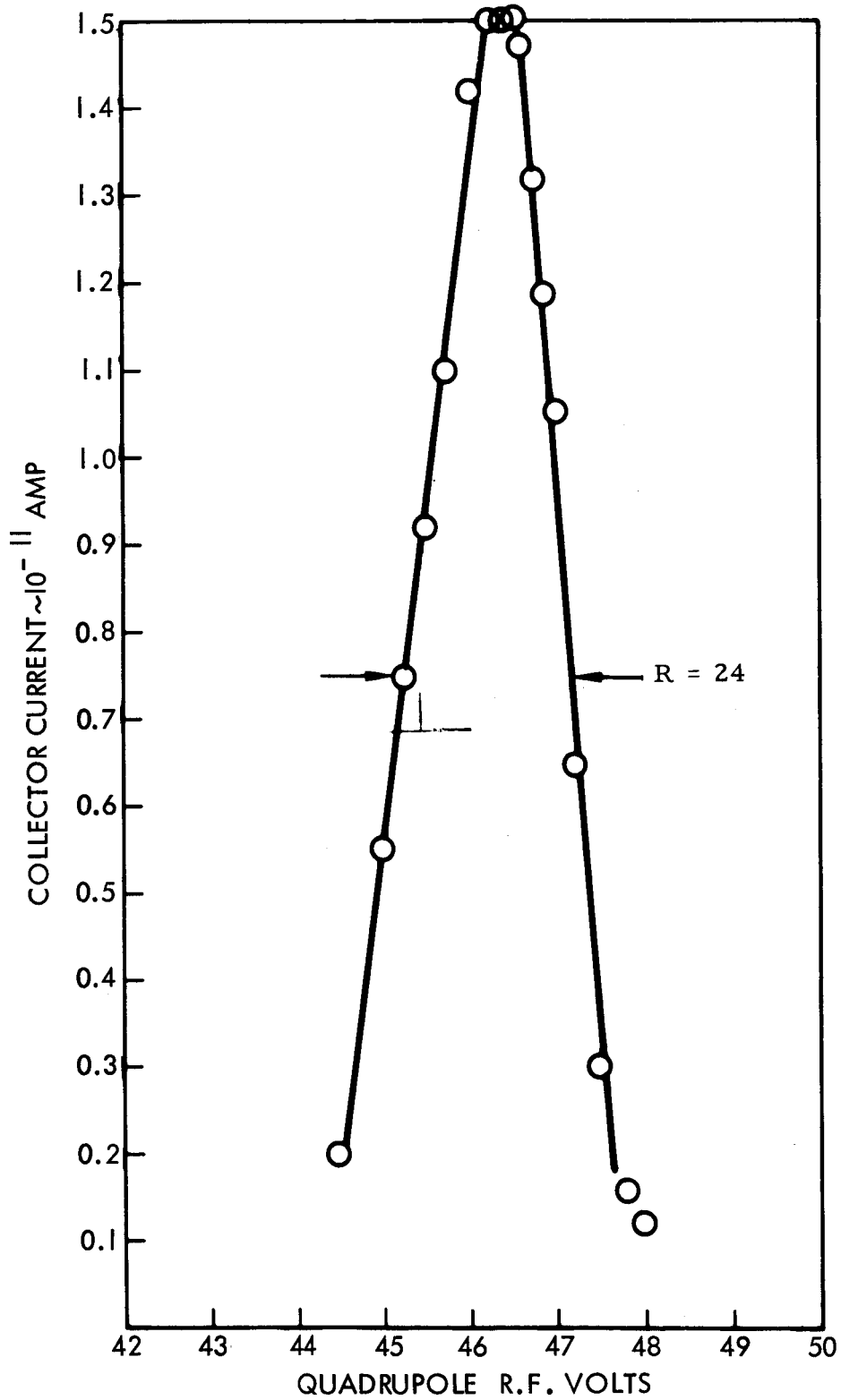
Figure 5.   Argon Resolution Curve for U/V Ratio of 0.153
(R = 24, Faraday Cup Detector)
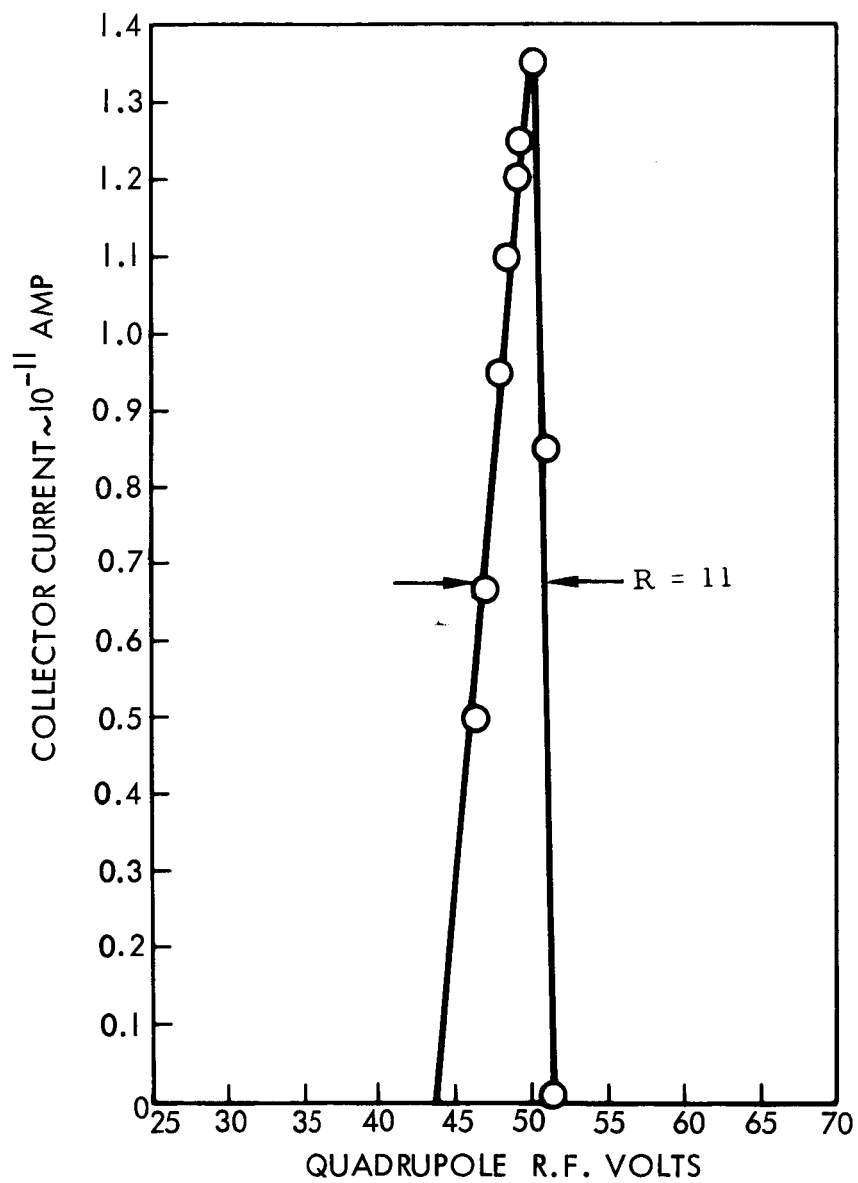
Figure 6. Argon Resolution Curve for U/V Ratio of
0.11 (R = 11, Faraday cup detector)
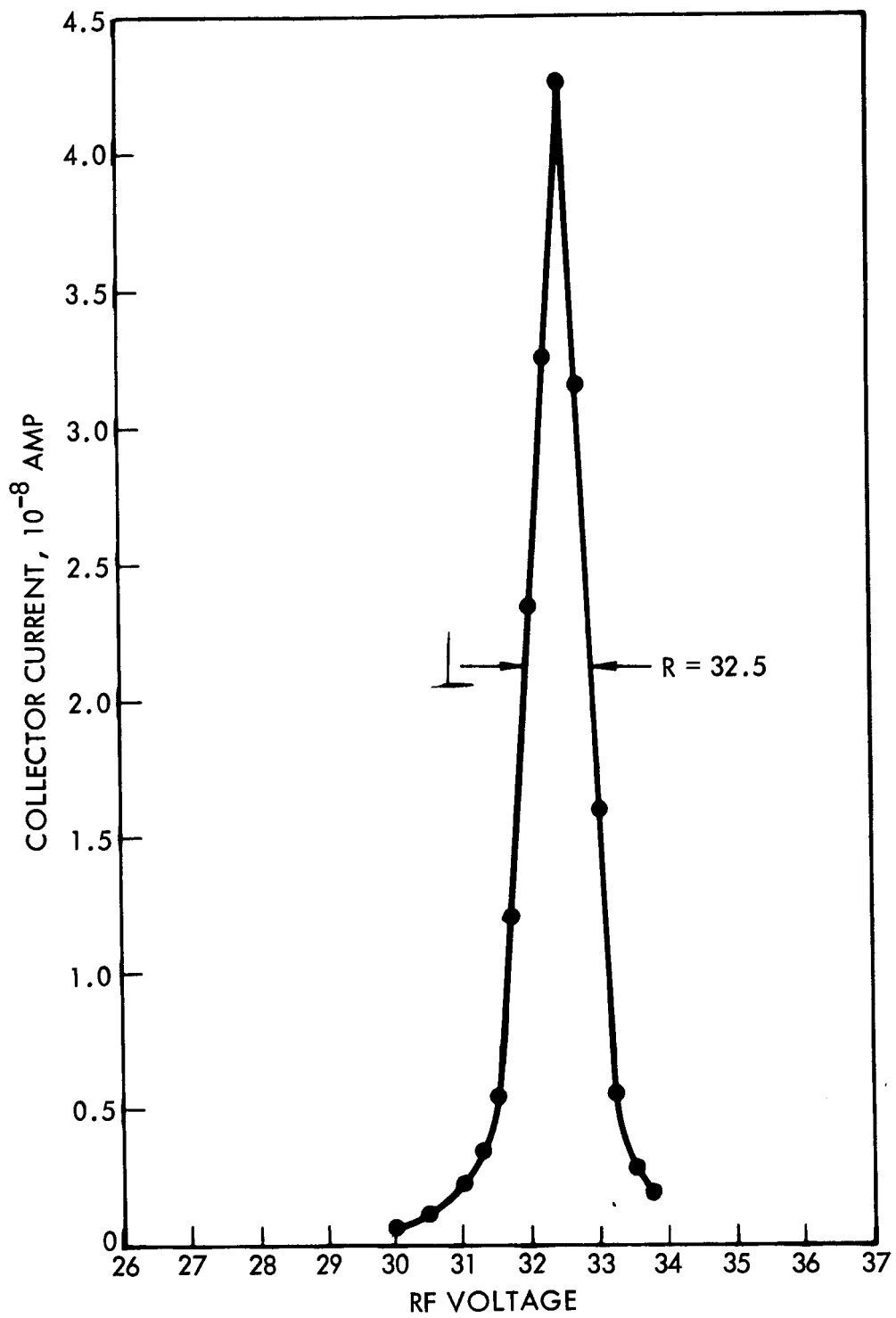
Figure 7. Molecular Nitrogen Ion Resolution Curve
for a U/V Ratio of 0.153 (R = 32,
SEM detector)
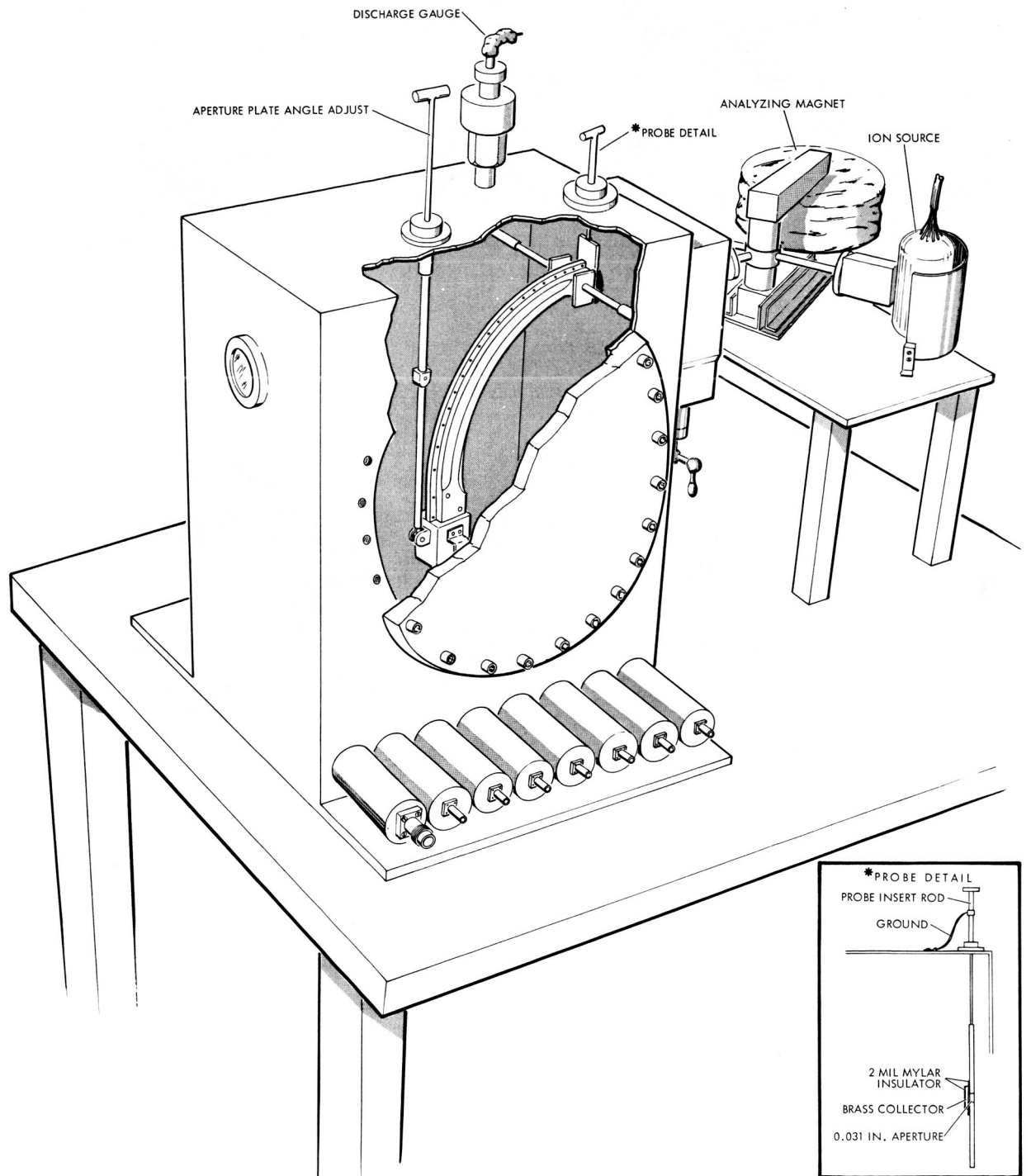
Figure 8. Experimental Configuration for Testing Quadrupole Spectrometer
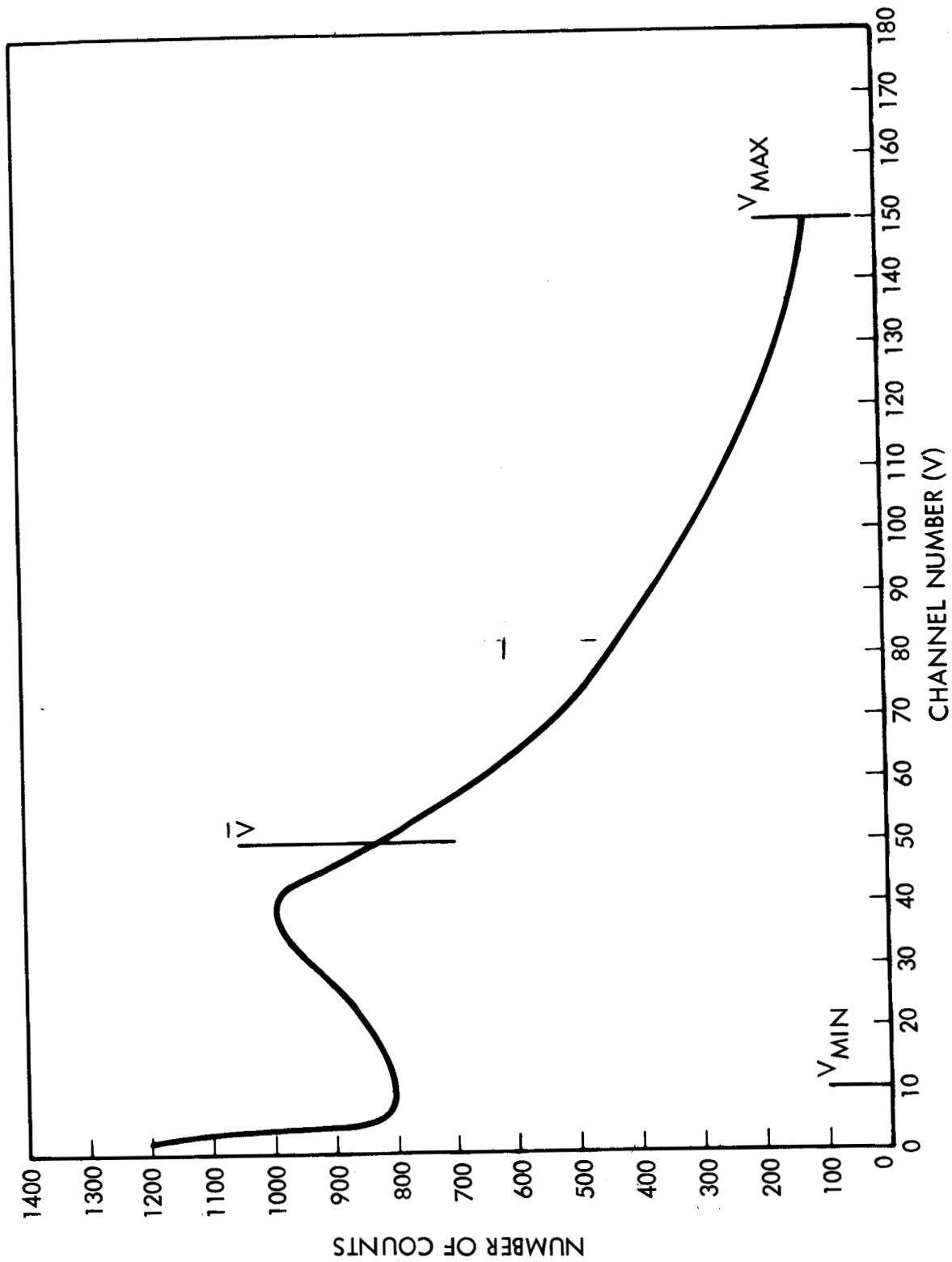
Figure 9. Differential Pulse Height Distributions for N_2^{28} Ions From an SEM Detector

FOCUSING MIRROR

TO PUMP

LiF WINDOW

POSITION
OF ELECTRON
MULTIPLIER
OR SPECTROMETER
APERTURE

SLIT

48000° K
PULSED
LIGHT SOURCE

VACUUM
CHAMBER

Figure 10. Light Transmission Test Configuration

Figure 11. Photo of Experimental Test Apparatus

NEW CONCEPTS

A patent disclosure is being submitted on the curved electric quadrupole mass spectrometer which is the subject matter of this report and which represents a new concept in the design and use of this instrument.

APPENDIX A

THEORY OF THE CIRCULAR QUADRUPOLE SPECTROMETER

In order to prevent the direct photon flux from arriving at the ion detection surface, we propose to bend the quadrupole electrodes along a radius of curvature R_o, where $R_o \gg r_o$. Let $r(t)$ denote the plane polar displacement of an ion with respect to the center of curvature, and let y be its displacement normal to the plane of curvature. Then the Lagrangian for the ion can be written

$$L = \frac{1}{2} m \dot{r}^2 + \frac{1}{2} m \dot{y}^2 + \frac{1}{2} m r^2 \dot{\theta}^2 - eV(r, y, t)$$

where $V(r, y, t)$ is the quadrupole voltage. If we compute the equations of motion

$$\frac{d}{dt} \frac{\partial L}{\partial \dot{q}_j} - \frac{\partial L}{\partial q_j} = 0$$

we have

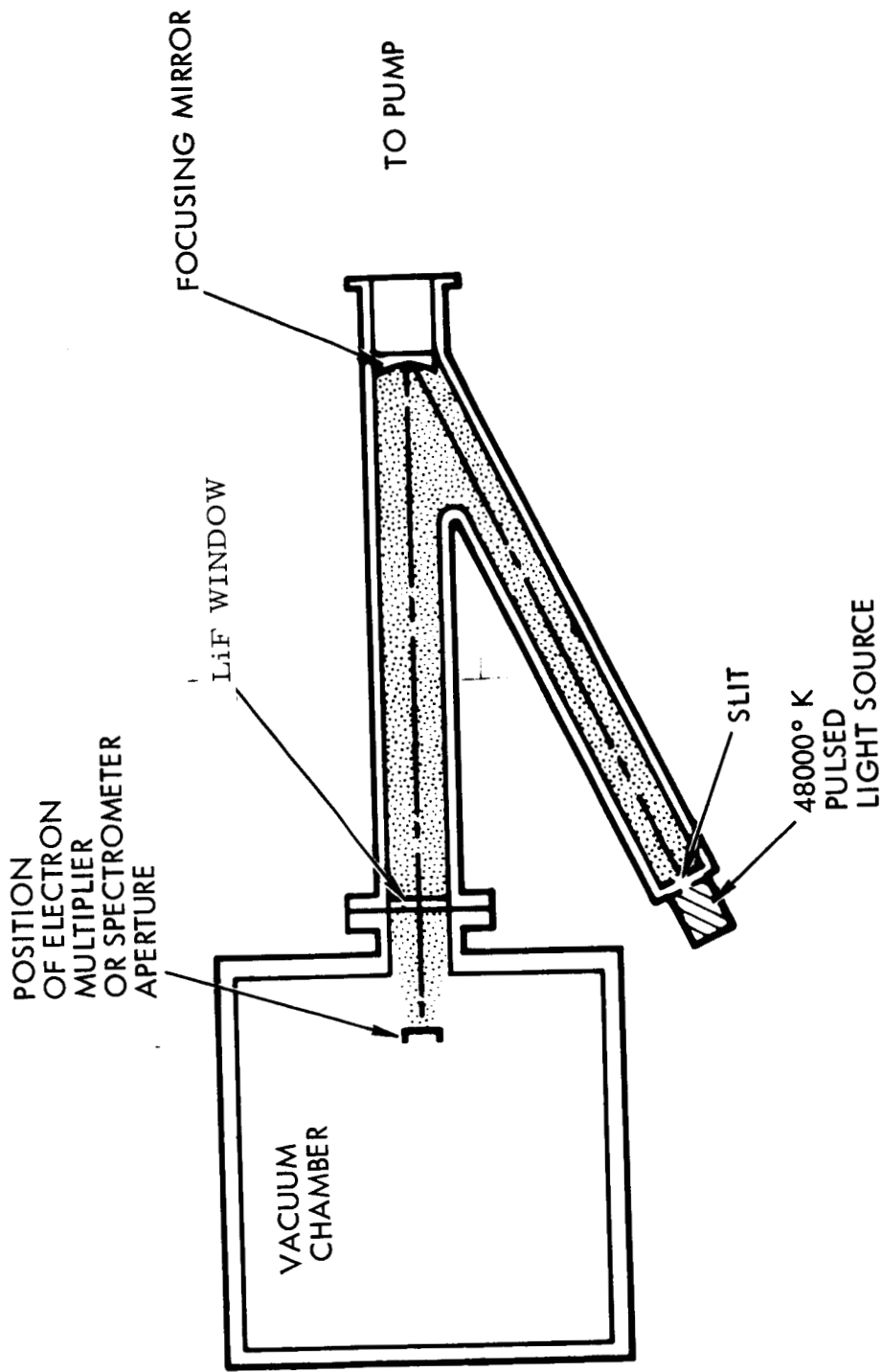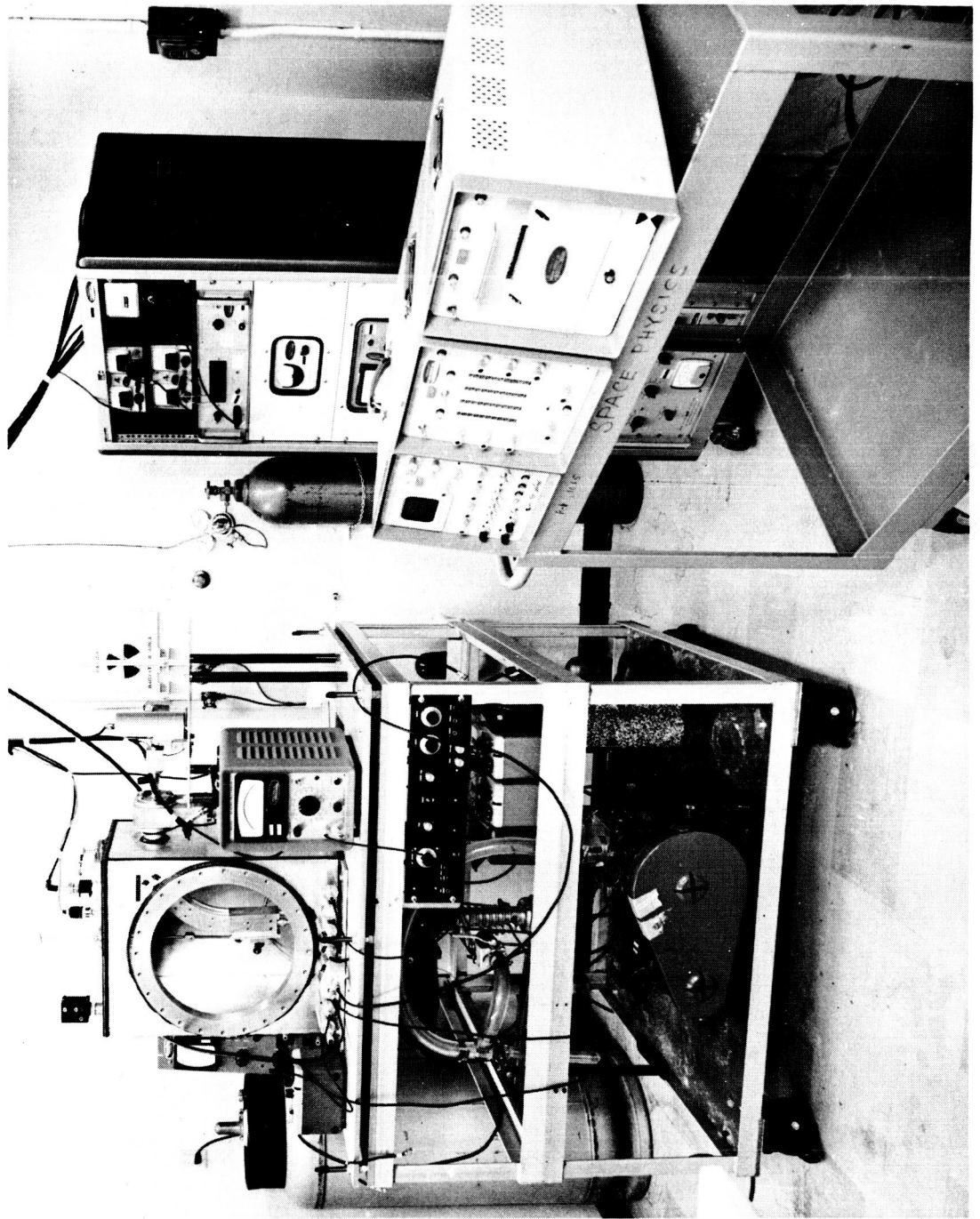$$m\ddot{r} - mr\dot{\theta}^2 + e \frac{\partial V}{\partial r}(r, y, t) = 0$$

$$\frac{d}{dt}(mr^2 \dot{\theta}) = 0$$

$$m\ddot{y} + e \frac{\partial V}{\partial y}(r, y, t) = 0$$

In the same spirit as that involved in calculating betatron oscillations in a strong-focusing particle accelerator, we introduce a radial excursion $x = r - R_o$ from the circular equilibrium orbit, where $0 \leq |x| \leq r_o \ll R_o$. The linearized equations of transverse motion to first order in x are then

$$m\ddot{x} + \left(6\xi_o / R_o^2 \right) x + e \frac{\partial V}{\partial x}(x, y, t) = 2\xi_o / R_o$$

$$m\ddot{y} + e \frac{\partial V}{\partial y}(x, y, t) = 0$$

$$\xi_o = \frac{1}{2} m v_\theta^2 \Big|_{t=0} = \frac{1}{2} m R_o^2 \dot{\theta}_o^2 = \text{kinetic energy of injection}$$

where ξ_o is determined by the constant of motion $(mr^2 \dot{\theta})$.

If we introduce the field potential

$$V(x,y,t) = (U_o + V_o \cos \omega t) \cdot (x^2 - y^2)/r_o^2$$

then

$$m\ddot{x} + 2\left(\frac{eU_o}{r_o^2} + 3\frac{\xi_o}{R_o^2} + \frac{eV_o}{r_o^2} \cos \omega t\right) x = 2\xi_o/R_o$$

$$m\ddot{y} - 2\frac{e}{r_o^2}(U_o + V_o \cos \omega t)\, y = 0$$

If one sets

$$a_x = 8\left(\frac{eU_o}{r_o^2} + 3\frac{\xi_o}{R_o^2}\right)/m\omega^2$$

$$a_y = 8e\, U_o/mr_o^2\omega^2$$

$$q = 4e\, V_o/mr_o^2\omega^2$$

$$\xi = \omega t/2$$

we have the two canonical Mathieu equations

$$\frac{d^2x}{d\xi^2} + (a_x + 2q \cos 2\xi)\, x = 8\xi_o/m\omega^2 R_o \approx 0$$

$$\frac{d^2y}{d\xi^2} - (a_y + 2q \cos 2\xi)\, y = 0$$

and the stability-instability properties of these equations yield the e/m passband of the curved instrument. The rhs of the equation governing the x-directed motion, can be written as

$$8\xi_o/m\omega_o^2 R_o = \frac{8\xi_o}{m\omega^2 R_o^2} \cdot R_o$$

A-2

For a mass $m = A(1.6 \times 10^{-24}$ gm) where A is in amu, one computes

$$mR_o^2\omega^2 = A(1.6 \times 10^6 \text{ eV})$$

and it follows that for $\xi_o \simeq 80$ eV, $A = 40$ amu (argon)

$$8\xi_o/m\omega^2 R_o^2 \simeq 10^{-5}$$

and

$$(8\xi_o/m\omega^2 R_o^2) \cdot R_o \sim 2 \times 10^{-4} \text{ cm}$$

This "displacement" is to be compared to the diameter of the entrance aperture, which is $d \sim 0.079$ cm $= 790 \times 10^{-4}$ cm. The stability of the x-motion is thus nearly independent of the orbital angular momentum of the ion. The two d-c parameters a_x and a_y are now different numerically, in contradistinction to the geometrically linear device. This simply alters the well-known stability "necktie" plot. However, for modest injection energies ξ_o (as envisaged for the instrument we shall use), it is readily verified that $a_x \approx a_y$, and one can still use the design formulas given by Paul for his linear device where $a_x = a_y$.

A-1. DESIGN CONSIDERATIONS

A-1.1 Resolution

Two important considerations determine the desirable upper and lower resolution limits. First, the measurement on relative abundances of Ne^{20} and Ne^{22} requires that the resolution be at least 11. Second, the expected low concentration of Kr^{82}, Kr^{83}, and Kr^{84} makes it desirable to sum over these three isotopic masses. This requires a resolution somewhat inferior to 4 1. We have selected $R = M/\Delta M = 25$ as a suitable intermediate value.

A-1.2 Field Radius and Entrance Aperture Diameter

It is desirable to keep the field radius r_o fairly small to reduce both weight and RF voltage requirements. The value $r_o = 0.4$ cm has been selected. This fixes the entrance aperture diameter ϕ through the relation $\phi = r_o/\sqrt{R} = 0.08$ cm. These dimensions should be within a ±1 percent tolerance.

A-1.3 Oscillator Frequency

It is desirable to keep the frequency as low as possible to reduce the RF power required by the spectrometer, as well as peak RF voltages on the electrodes. However, the minimum length of the spectrometer is inversely proportional to the frequencies. A frequency of 1.0 Mc was chosen as a suitable compromise, and must be stabilized to within ±1 percent.

A-1.4 RF and DC Voltages

The maximum RF and DC voltages are required for the mass selection of Kr^{83}. For a mass peak centered on Kr^{83} one finds a maximum RF voltage of V_o = 95.9 volts and an associated DC voltage, U_o = 16.1 volts, regulated to within about ±2 percent.

A-1.5 Spectrometer Length

The path length along the curved axis of the spectrometer must be sufficient to provide a minimum of 3.5 R $\cong$ 18 high frequency oscillations of the selected ion.

A-1.6 RF Power Requirement

The maximum power drawn by the spectrometer from its RF oscillator will occur during the selection of Kr^{83}. This will be $6.54 \times 10^{-4} A^2 f^5 r_o^4 C/Q$. A pessimistic estimate of capacitance is 200 μμf and of Q is 20. Then the maximum r-f power would be 285 milliwatts.

A-1.7 Estimates of a_x and a_y

For the circular analyzer one can write

$$a_x = a_y \left(1 + 3 r_o^2 \Phi_o / R_o^2 U_o \right)$$

$$a_y = 4 e U_o / r_o^2 M \omega^2$$

The minimum mass to be analyzed is N^+, A = 14, which requires U_o = 2.7 volts. It follows that this is the worst possible deviation of

a_x from a_y, and one has, for Φ_o = 80 volts injection energy, r_o = 0.4 cm, R_o = 20 cm, U_o = 2.7 volts,

$$a_x = 1.0358 \, a_y$$

which is an insignificant correction when one requires as low resolution as 25. One is therefore justified in using Paul's design formulas for the geometrically linear quadrupole filter.

A-1.8 Operation as Total Ion Trap

The operation of the spectrometer with only an r-f voltage, i.e., U_o = 0, leads to selection of all mass from 1 amu to an upper limit fixed by the peak RF voltage. Thus, for the total ion concentration measurement, one requires U_o = 0, V_o = 95.9 volts which will record the sum of masses 1-83 atomic mass unit.

A simplified schematic of the proposed spectrometer is shown in Figure 2. It should be noted that the geometrical entrance aperture is 5×10^{-3} cm^2. It is not expected that a pre-acceleration grid in front of the entrance aperture will result in a significant reduction in the entrance aperture. It should also be pointed out that significant increases in the effective aperture and therefore sensitivity can be made if the measurements are limited to masses below 40 atomic mass units.

APPENDIX B

LIGHT INTENSITY CALCULATIONS

B-1 PHOTON INTENSITY AT SPECTROMETER APERTURE

The vacuum ultraviolet light source used to test the photoelectric response of the quadrupole sensor-secondary emission multiplier detector has an equivalent blackbody temperature of 48,000 $^{\circ}K$ and a radiating surface area in the form of a slit 200 microns wide and 3.175 millimeters long. By means of a spherical mirror, this area is effectively imaged at a distance D = 17 inches (43.2 centimeters) from the entrance aperture of the mass filter.

The total number of photons of wavelength λ emitted by unit area of a blackbody at temperature T per unit wavelength is

$$n(\lambda) = \frac{A}{hc} \lambda^{-4} \left[\exp (\beta c/\lambda) - 1 \right]^{-1}$$

where

$$A = 3.74 \times 10^{-5} \text{ erg-cm}^3 - \text{sec}^{-1}$$

$$\beta = h/kT$$

If one defines $x = \beta c/\lambda$, then the total flux of photons between two wavelengths λ_1 and λ_2 is

$$\Phi(\lambda_1, \lambda_2, T) = (A/hc^4\beta^3) \int_{x_2}^{x_1} \frac{x^2 e^{-x}}{1 - e^{-x}} \, dx$$

where

$$x_{1,2} = \beta c/\lambda_{1,2}$$

If we choose $\lambda_1 = 1200 \text{ Å}$, $\lambda_2 = 3000 \text{ Å}$, $T = 4.8 \times 10^4 \, ^{\circ}K$, then $x_1 = 2.5$, $x_2 = 1.0$ and one has

$$\Phi_0(1200 \text{ Å}, 3000 \text{ Å}, 48,000^{\circ}) = \frac{Ak^3 T^3}{h^4 c^4} \int_{1.0}^{2.5} \frac{e^{-x}}{1 - e^{-x}} x \, dx \text{ , photons -cm}^{-2} \text{-sec}^{-1}$$

The integral has been evaluated numerically, and has the value 0.93. Thus

$$\Phi_o = 0.93 \ Ak^3 T^3 / h^4 c^4 \quad photons\text{-}cm^{-2}\text{-}sec^{-1}$$

From the geometry of the light source, mirror and mass filter arrangement, one can write down the flux at the entrance aperture as

$$\Phi_1 = \frac{area\ of\ source}{2\pi D^2} \ \Phi_o \simeq (6 \times 10^{-7}) \ \Phi_o \quad photons\text{-}cm^{-2}\text{-}sec^{-1}$$

At $T = 4.8 \times 10^4 \ {}^oK$, $\Phi_o = 6.8 \times 10^{24}$ photon-cm^{-2}-sec^{-1}. Thus $\Phi_1 \sim 4 \times 10^{18}$ photons-cm^{-2}-sec^{-1}.

This value of the flux has been calculated on the assumptions that (1) the mirror has unity reflectance between $1200 \ \overset{o}{A} \lesssim \lambda \lesssim 3000 \ \overset{o}{A}$; (2) the virtual source (image source) radiates into a 2π solid angle. Both assumptions are questionable, but the combined error due to these factors would likely not reduce the computed value of Φ_1 by more than a factor of 2 to 3.

The total number of photons entering the quadrupole aperture (area of $5 \times 10^{-3} \ cm^2$) in a light pulse of e-folding time $t_o = 2 \ \mu sec$ is

$$n_{ph} = \Phi_1 t_o \times 5 \times 10^{-3} = 4 \times 10^{18} \times 5 \times 10^{-3} \times 2 \times 10^{-6}$$

or

$$n_{ph} = 4 \times 10^{10} \ photons$$

APPENDIX C

RF-DC POWER SUPPLY UNIT

C-1 SPECIFICATIONS AND CONTROL FUNCTIONS

Output Frequency

1 megacycle crystal controlled

Crystal frequency can be changed ±10 cps about 1 Mc

Laboratory test indicates a drift of less than 2 cps in 8 hours under normal room ambient temperature conditions.

Output Amplitude — AC (Push Pull)

Continuously variable in one range from 2 volts peak to 100 volts peak into a capacitive load. May be increased to 120 volts peak with a resistor change in the summing network.

Output Amplitude AC Balance

Push pull signals may be unbalanced ±5 percent with the balance adjust control. Because of the nature of the amplitude stabilization circuitry the balance adjust control has approximately 10 times the effect on the - rail AC signal amplitude.

Tuning Range

A tuning range of ±25 μμf maximum is available with the tuning control to allow for increases or decreases of load capacitances due to cable length changes, spectrometer changes, etc.

Tuning is performed by using a suitable DC voltmeter connected to the tune monitor jacks and "tuning for maximum."

Output Amplitude — DC (+ Rail, - Rail)

Continuously variable from 0.00 to 0.20 times the peak AC rail voltage. The positive DC potential is added to the + rail AC and the negative DC potential is added to - rail AC.

Spectrometer External Load

+ Rail to ground load	156 μμf
- Rail to ground load	156 μμf
+ Rail to - rail load	34 μμf

(These loads, cables, rails, etc., are required to form an operational unit.)

Output Amplitude Stability — AC

Better than 0.01 percent/hr at 100 volts peak and 0.05 percent/hr at 10 volts peak with fixed loads, under normal laboratory line variations and room ambient temperature conditions.

Output Amplitude Stability — DC

Same as AC

Output Amplitude AC Detector Accuracy

Calibrated against Fluke thermal transfer converters to better than 0.05 percent at 55 volts peak AC.

Output Amplitude AC Detector Tracking Linearity

Better than 0.05 percent from 20 volts peak to 55 volts peak.

Output Amplitude AC Peak Voltage to Detector Voltage Conversion Factor

Detector voltage x 1.030 = AC peak voltage

May be changed to 1.000 at reduced accuracy ($\sim$ 0.5 percent) with resistor change.

Main Amplitude Control

Sets the amplitudes of the AC rail voltage from approximately 1 volt to 100 volts peak. With the fine amplitude control in the full clockwise position, the peak AC + rail voltage may be set to within approximately 3 percent directly from the dial reading.

Fine Amplitude Control

Approximately 1 percent full scale range. Simplifies setting exacting amplitudes at lower levels.

External Internal Switch

Switches the spectrometer from its internal AC amplitude control to an external control.

Sweep Centering

Sets the nominal AC amplitude about which the external amplitude control or sweep operates.

External Sweep

The external amplitude control signal may be in the form of DC or AC not to exceed 20 cps. With the main amplitude control in its maximum clockwise position, an external AC signal of approximately 30 volts peak to peak will vary the spectrometer AC output amplitude over a range of 10:1, i.e., 100 volts to 10 volts peak. By decreasing the main amplitude control to 1/10 full scale the spectrometer amplitude can be varied from approximately 10 to 1 volt peak.

C-2 OPERATING INSTRUCTIONS

1. Connect the spectrometer exciter to the two HP 721 A power supplies. The power supplies should be set to + and - 25 volts ±1 percent.

2. Connect the spectrometer exciter to the rail assembly with the interconnecting cables provided.

    Note

    The cable and rail assembly capacitances are tuned and should not be changed. If cable or rail assembly changes are to be made which results in a capacitance change of greater than ±20 μμf, the spectrometer exciter must be properly compensated for by adding, or removing, fixed capacitors within the unit.

3. Connect the Simpson voltmeter to the tune jacks. Set the internal-external switch to internal, turn on power.

4. Adjust the tune control for a maximum reading on the Simpson voltmeter. The voltage indicated by the Simpson voltmeter should be approximately +1 volt. A negative voltage will be indicated if the unit is poorly tuned or excessively loaded.

5. After tuning, the peak AC rail voltage may be set to the desired amplitude with the main amplitude control. The + AC rail amplitude may be set to within 3 percent directly from the main amplitude dial reading. To obtain a more precise reading of the peak AC rail voltage, connect a digital voltmeter (HP 344 A, or equivalent) to the + AC rail monitor jacks, the voltage indicated by the digital voltmeter multiplied by 1.030 is equal to the peak AC rail voltage.
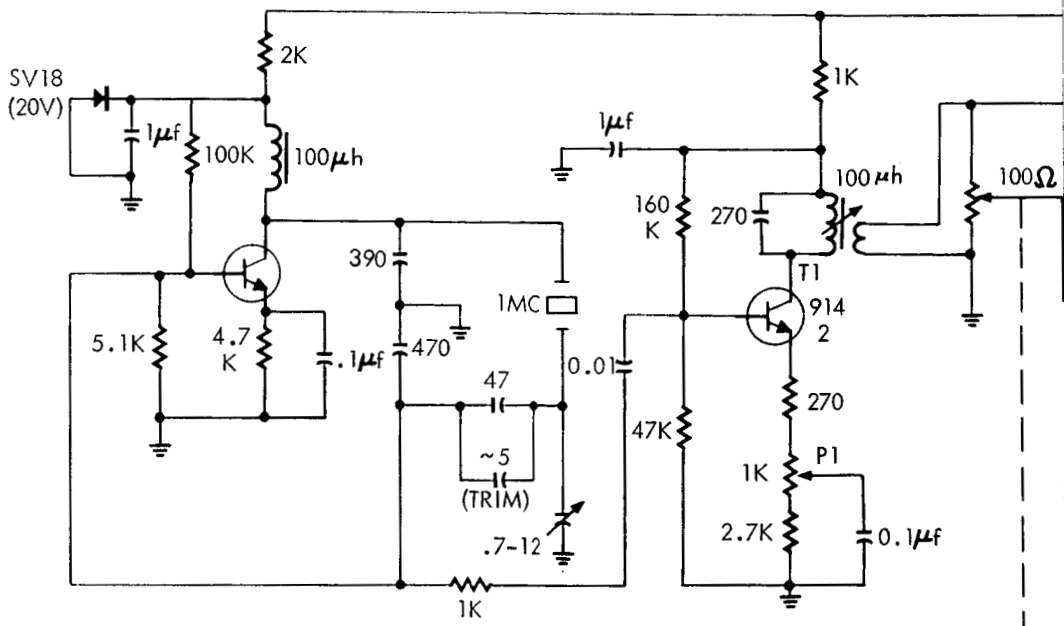
    Note

    When measuring the rail monitor with the digital voltmeter, the 10.2 meg voltmeter load simulator should be removed. For the most accurate reading the fine control should be in, or near, its maximum clockwise position.

After setting the + AC rail to the desired amplitude connect the digital voltmeter to the - rail monitor and adjust the balance control for the same amplitude. It should be noted that the balance control has a range of about 5 percent and requires very small incremental movements when making very precise balance adjustments. Since there is some interaction between the balance control and the + rail AC voltage, the + rail monitor voltages should be rechecked.
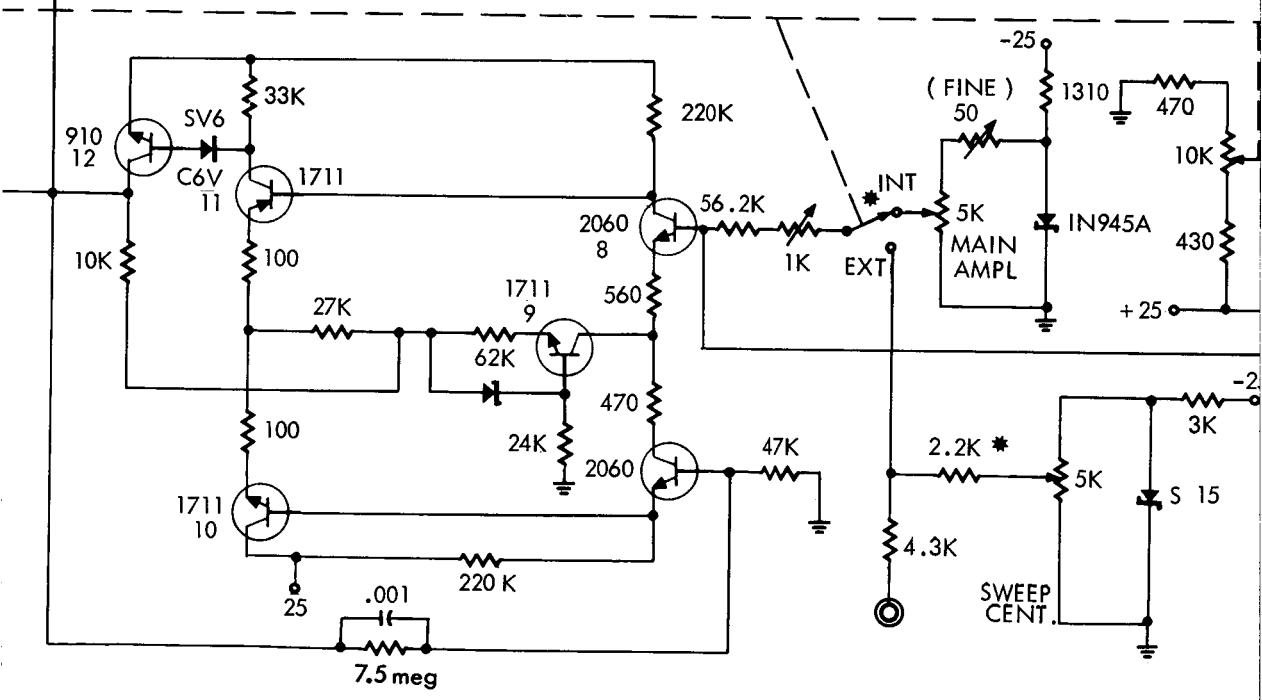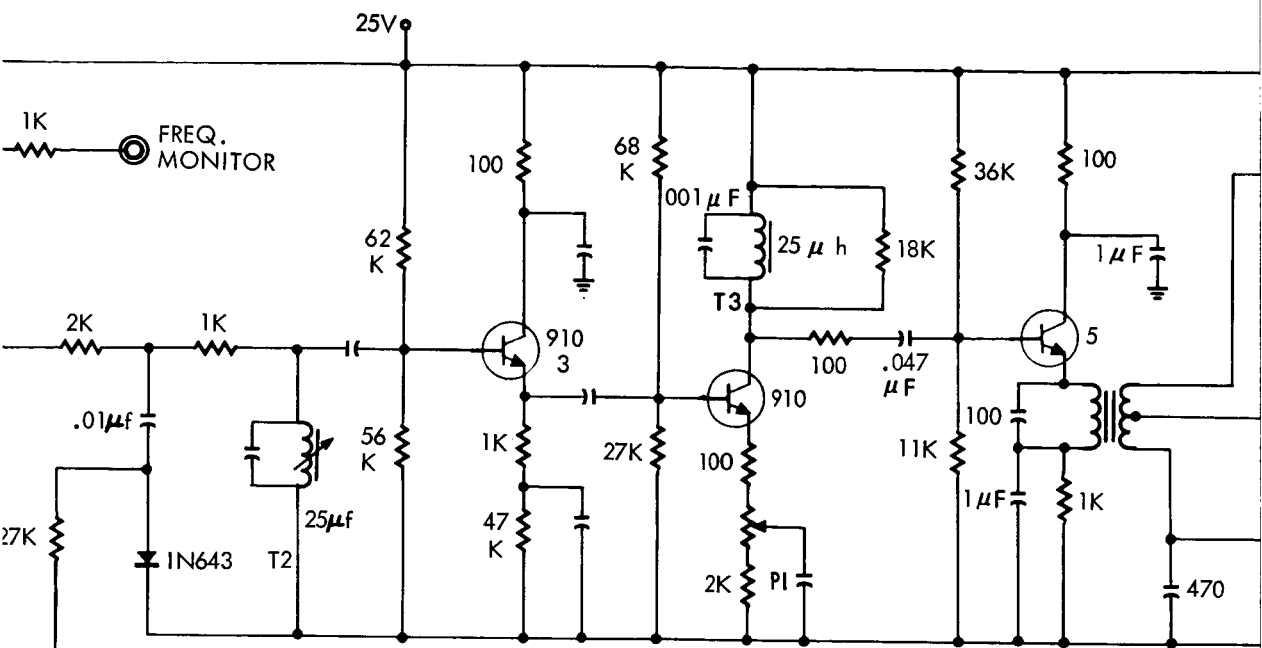
6. After the balance adjustments have been made the spectrometer will maintain its balance with moderate accuracy over its range of 10 volts to 100 volts, but should be rechecked and adjusted if necessary when precision measurements are to be made.

7. The + and - slope DC voltages may be applied to the rails to the desired levels by adjusting the appropriate slope potentiometer. The slope potentiometers have been calibrated such that when a slope potentiometer is in its full scale (maximum clockwise) position, the DC voltage applied to its rail has an amplitude which is equal to 0.20 times the peak AC voltage existing on that rail. If desired, these voltages may be measured at the slope test jacks. These voltages are derived from a relatively high impedance source and, to maintain calibration, should be measured with an infinite impedance differential type of voltmeter.

8. To obtain the best possible performance accuracy from the spectrometer exciter the following operating procedures should be observed:

    a) When making small amplitude changes at low levels, it may be more desirable to use the fine amplitude control; however, when making very precise measurements this control should be kept near its full clockwise position.

    b) The tuning adjustment should be checked periodically to assure proper tuning, and should always be checked when making large changes in the AC rail amplitudes.

    c) When measuring the + and - AC rail monitor voltages the total resistive load including the voltmeter load should be 10.2 megs.

    d) Certain types of digital voltmeters, not having the automatic polarity reversing feature as well as certain types of differential voltmeters when used to measure negative potentials, introduce considerable hum into the measuring circuit which can introduce some error. If these types of voltmeters are to be used to measure the - rail monitor or - slope voltages, the voltmeter should be bypassed with a low leakage bypass capacitor of approximately 1 μf, but should be removed when the spectrometer is used in the sweep mode at frequencies about 1 cps.

e) The original spectrometer specifications called for a voltage generation capability of 10 to 100 volts peak. Though the spectrometer output voltages can be set to as low as 1 volt peak, no performance tests have been made below 10 volts peak; it is believed, however, that stability and readout accuracy will become rapidly degraded for amplitude levels below 5 volts peak and should be considered by the operator when operating the spectrometer in this area.

* FRONT PANEL CONTROLS

25V

1K FREQ. MONITOR

100   68 K   001 µF   25 µ h   18K   T3   36K   100   1 µF

62 K

2K   1K   910 3   910   100   .047 µF   5

.01µf   56 K   1K   27K   100   100   11K   1µF   1K

27K   IN643   T2   25µf   47 K   2K   P1   470

-25   (FINE)   1310   470
        50
910 12   SV6   33K   220K   10K
C6V 11   1711   INT   IN945A   430
10K   100   56.2K   5K MAIN AMPL   +25
    27K   1711 9   560   1K   EXT
    62K   470   -2
    100   24K   2060   47K   2.2K *   3K
1711 10   2060   4.3K   5K   S 15
25   .001   220 K   SWEEP CENT.
7.5 meg

2
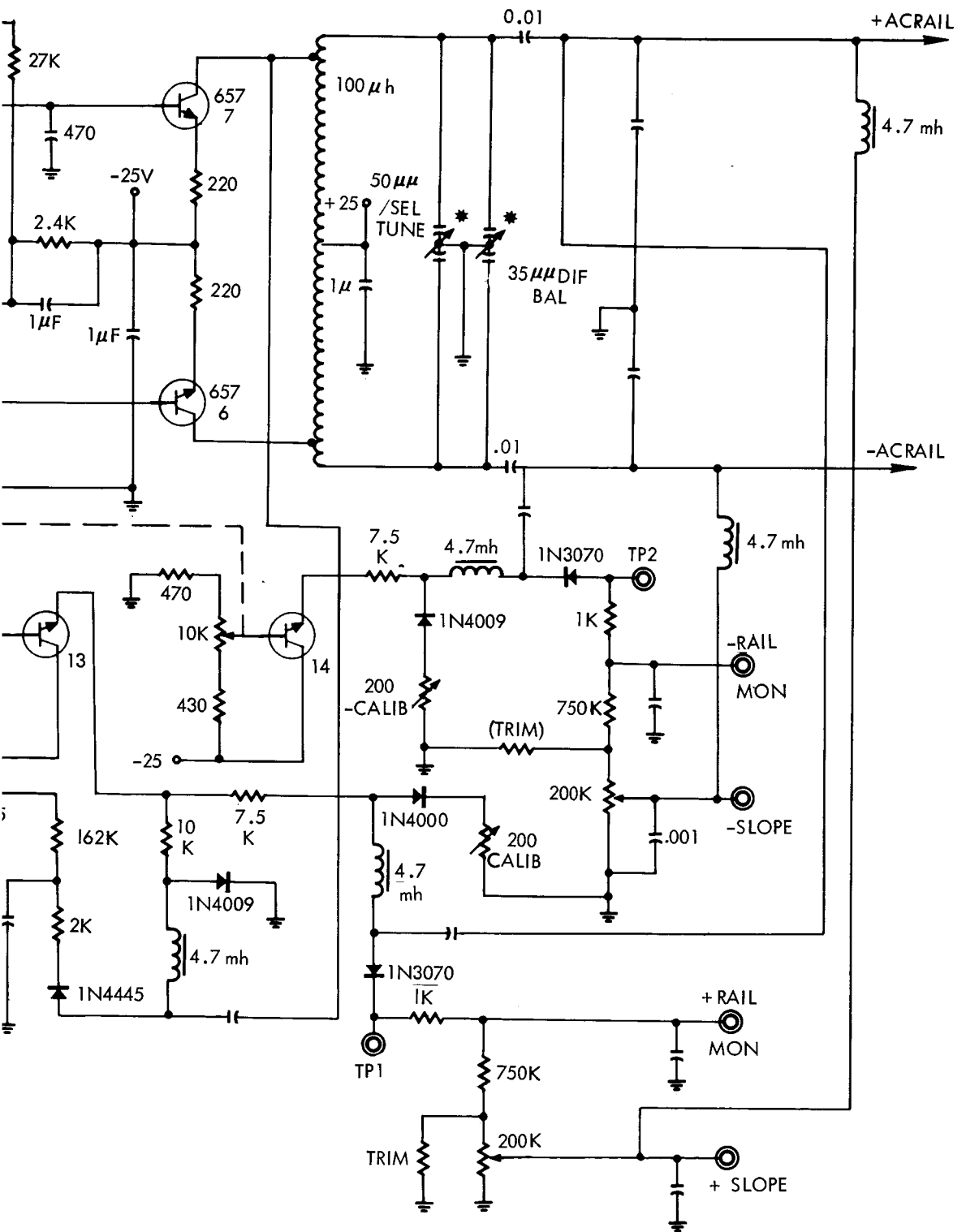
Spectrometer RF - DC Power Supply

DRAWING NO

SHEET

D

C

TABULATION

DASH NO.	DIM A	MATL -TUBING
-3	7.350 R	6061-T6 .375 OD x .25 ID
-4	7.860 R	6061-T6 .375 OD x .25 ID
-5	8.370 R	6061-T6 .375 OD x .25 ID
-6	7.350 R	6061-T6 .375 OD x .31 ID
-7	7.860 R	6061-T6 .375 OD x .31 ID
-8	8.370 R	6061-T6 .375 OD x .31 ID

'A'

90°

SCALE : 1/2

.62

.375

.250

.12 DIA

2.00 SQ

.625 DIA

.125

.562

1.625 DIA

1.750 SQ

1.875 SQ

.062

.125

.125

.187 REF

.125 DIA 2 HOLES
C'SK FARSIDE
FOR #4 100° SCREW
TYP 4 SIDES

B

- 9 FRONT CAP

9

10

.20

.105

A

PRESS FIT -9 & -10
TAP 10-32 .12 FULL THREAD
N-3
DRILL .090 DIA HOLE N-3 & -10

ASSY OF -9 & -10

I

.187

.125

.375 DIA

.625 DIA
PRESS FIT
WITH -9

.625 DIA —
PRESS FIT
WITH -9

-10 RETAINER

.031 ± .001 DIA

.375 DIA
PRESS FIT WITH -10

- 11 COLLIMATOR

.375 ID x .395 OD
x .25 WIDE

.20

-12 INSULATOR

—.187

.25

1.28 TYP
LINEAR DIM

TAP 6-32 THRU 19 PLACES
IN -1 ONLY
DR'LL .141 DIA THRU
-2
MATCH -1 & -2

A

A

2.00
CONST

2.62
CONST

8.76 R
GROOVE
SEE SECT A-A

6.95 R
GROOVE

6.70 R

9.00 R   7.860 D

6.86 D

6.54 R

REF
1.625
CONST

.250

7.048 R

.25
TYP

.38 TYP

90

1.875

.937

1.750

.875

.12
TYP

.562

1.000

.06 R
TYP

.562
TYP

.812 R

1.125
TYP

—TAP 4-40 .12 PERFECT THREA
DRILL .25 DEEP
DO NOT BREAK THRU
4 PLACES BOTH ENDS

② 2

⑮ 19 REQD

① 1

.028 +.002
-.000

.080

.005 R
TYP
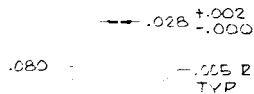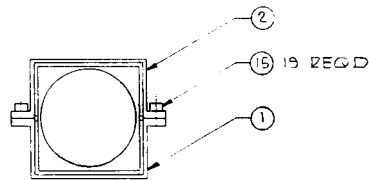
.395 R
REF

SECTION A A
GROOVE DETAIL
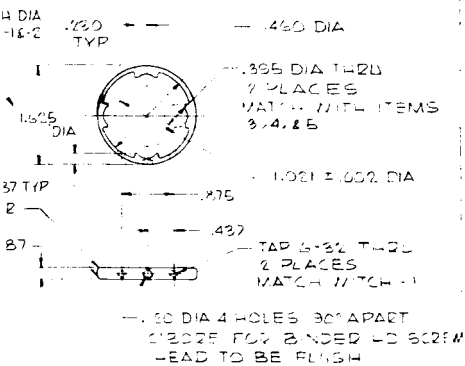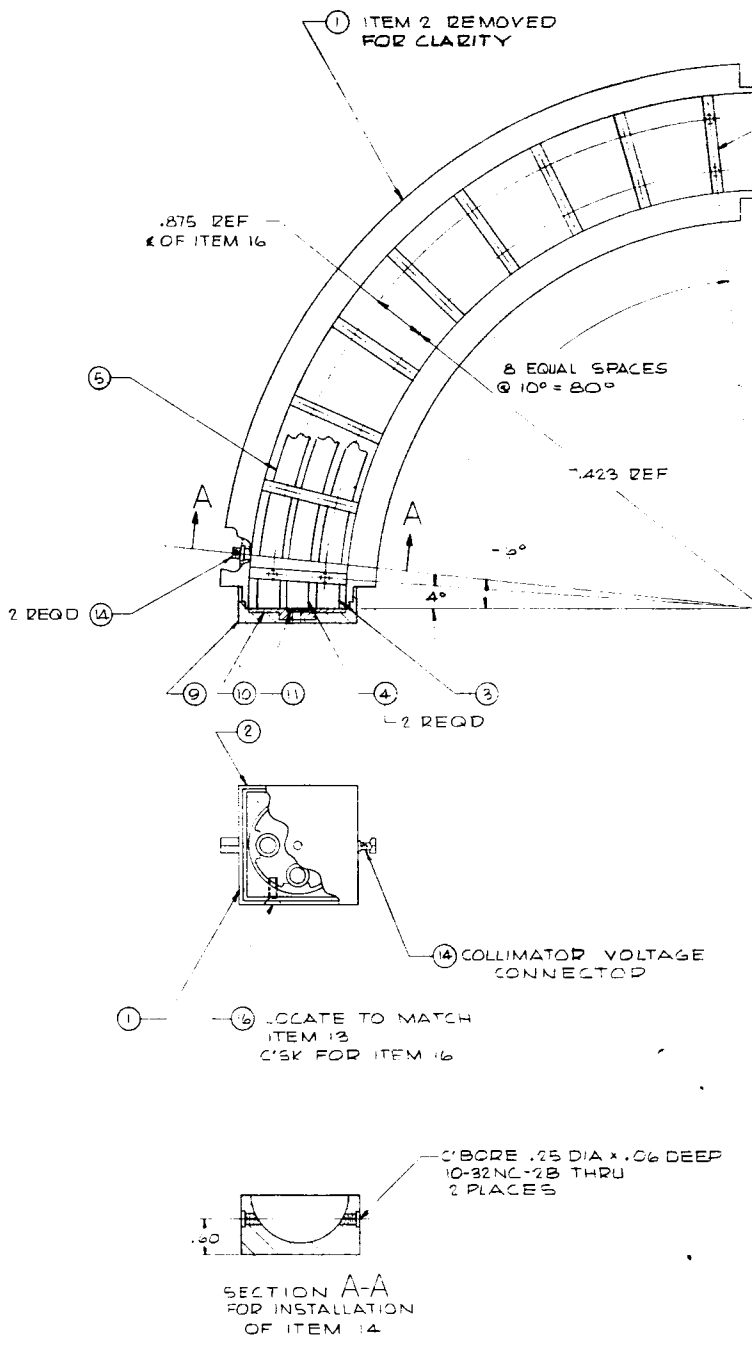
.480 DIA

.130
TYP

.395 DIA THRU
2 PLACES
MATCH WITH ITEMS
3, 4, & 5

1.625
DIA

.031 ± .002 DIA

.75

.437

TAP 6-32 THRU
2 PLACES
MATCH WITH -1

.20 DIA 4 HOLES 90° APART
C'BORE FOR BONDED HD SCREW
HEAD TO BE FLUSH

-13 RING

ITEM 2 REMOVED
FOR CLARITY

.875 REF —
⊄ OF ITEM 16

8 EQUAL SPACES
@ 10° = 80°

⊄.423 REF

⑤

A   A

6°

2 REQD ⑭

4°

⑨ ⑩ ⑪   ④   ③

└ 2 REQD

②

⑭ COLLIMATOR VOLTAGE
CONNECTOR

① —   ⑥ LOCATE TO MATCH
ITEM 13
C'SK FOR ITEM 16

— C'BORE .25 DIA × .06 DEEP
10-32NC-2B THRU
2 PLACES

T
.60
⊥

SECTION A-A
FOR INSTALLATION
OF ITEM 14

1. IDENTIFICATION MARKING IN ACCORDANCE WITH STL SPEC. PR 12-1
    TYPE____ CLASS.____PART NUMBER____
NOTES: UNLESS OTHERWISE SPECIFIED

					REVISIONS				
	ZONE	REV		DESCRIPTION			BY	DATE	CHK	APPROVAL

D

—⑬ 9 REQD

C

←

B

X215121

18	AB831-A-1	SCREW	6-32		ABSCOA IND UNISEAL SCREW		16
19		SCREW, CAP	6-32 x 1/4				15
3	*31-01	CONNECTOR			MICRODOT		14
5	-13	RING	.625 DIA x .188	6061-T6	QQ-A-327		13
20	-12	INSULATOR	.010 THK	NYLON			12
1	-11	COLLIMATOR	.062 THK	BRASS	QQ-B-626		11
1	-10	RETAINER	1.187 THK	EPOXY GLASS	MIL-P-18177		10
1	-9	CAP, FRONT	.62 THK	6061-T6	QQ-A-327		9
1	-8	ELECTRODES POSITIVE	.375 OD x .312 ID	6061-T6 ALUM TUBING	WW-T-789 (I)		8
2	-7	ELECTRODES NEGATIVE	.375 OD x .312 ID				7
1	-6	ELECTRODES POSITIVE	.375 OD x .312 ID				6
1	-5	ELECTRODES POSITIVE	.375 OD x .312 ID				5
2	-4	ELECTRODES NEGATIVE	.375 OD x .312 ID				4
1	-3	ELECTRODES POSITIVE	.375 OD x .250 ID	6061-T6 ALUM TUBING	WW-T-789 (1)		3
1	-2	HOUSING, UPPER		6061-T6	QQ-A-327		2
1	-1	HOUSING, LOWER		6061-T6	QQ-A-327		1

				PART NO	PART NAME	STOCK	MATERIAL	SPEC	CAT REF	CODE IDENT	ZONE	ITEM NO	USED ON	NEXT ASSY	HEAT ASSY	FINAL ASSY
				REQD PER NOTED ASSY			DESCRIPTION							APPLICATION		QTY REQD

CONFIGURATION   LIST OF MATERIALS

UNLESS OTHERWISE SPECIFIED

1 DIMENSIONING & TOLERANCING PER MIL-STD-8
2 DIMENSIONS IN INCHES TOLERANCES
   ANGLES ± 0° 30'
3 STC HOLE TOLERANCES PER AND10387
4 ALL OHMS TO APPLY BEFORE PLATING OR CONVERSION COATING
5 REMOVE BURRS & SHARP EDGES
6 SURFACE ROUGH
   MESS PER MIL-STD-10
7 RIVET CODING PER NAS 523
8 WELD SYMBOLS PER JAN STD-19
9 THREADS PER MIL STD 8, MIL S-7742 & MIL-P-7105
10 ELECTRICAL & ELECTRONIC SYMBOLS & REFERENCE DESIGNATIONS PER MIL-STD-15 & MIL-STD-16

APPLICABLE SPECIFICATIONS
THE ABOVE REFERENCED STL SPECS FORM A PART OF THIS DRAWING

FINISH

HEAT TREAT

DO NOT SCALE DRAWING

THE FOLLOWING E.O.'S HAVE BEEN ATTACHED TO THIS PRINT

STL APPROVALS

DRAWN	
CHECKED	
STRUCTURES	
MATLS & PROCESSES	
ENGR	
SUPERVISION	
SPECIAL	
OTHER APPROVALS	

TRW SPACE TECHNOLOGY LABORATORIES
ONE SPACE PARK · REDONDO BEACH · CALIFORNIA

ASSEMBLY - ELECTROSTATIC MASS SPECTROMETER

DWG SIZE	CODE IDENT NO	
J	11982	X215121

| SCALE 1/1 | WEIGHT | SHEET |

A

STL FORM 1405-R REV. 1-60